SERIES OF PYRIDINE-2,6-DICARBOHYDRAZIDE AROYL HYDRAZONE LIGANDS: SYNTHESIS, CHARACTERIZATION AND CRYSTAL STRUCTURES

M.Sc. Thesis

by

Ravi Kumar

DISCIPLINE OF CHEMISTRY

INDIAN INSTITUTE OF TECHNOLOGY INDORE

JUNE 2015

SERIES OF PYRIDINE-2,6-DICARBOHYDRAZIDE AROYL HYDRAZONE LIGANDS: SYNTHESIS, CHARACTERIZATION AND CRYSTAL STRUCTURES

A THESIS

Submitted in partial fulfillment of the
requirements for the award of the degree
of
Master of Science

by

Ravi Kumar

DISCIPLINE OF CHEMISTRY
INDIAN INSTITUTE OF TECHNOLOGY INDORE
JUNE, 2015

INDIAN INSTITUTE OF TECHNOLOGY INDORE

CANDIDATE'S DECLARATION

I hereby certify that the work which is being presented in the thesis entitled **SERIES OF PYRIDINE-2,6-DICARBOHYDRAZIDE AROYL HYDRAZONE LIGANDS: SYNTHESIS, CHARACTERIZATION AND CRYSTAL STRUCTURES** in the partial fulfillment of the requirements for the award of the degree of **MASTER OF SCIENCE** and submitted in the **DISCIPLINE OF CHEMISTRY, INDIAN INSTITUTE OF TECHNOLOGY INDORE**, is an authentic record of my own work carried out during the time period from July, 2014 to June, 2015 under the supervision of Dr. Shaikh M. Mobin, Assistant Professor, Discipline of Chemistry.

The matter presented in this thesis has not been submitted by me for the award of any other degree of this or any other institute.

Signature of the student with date
(Mr. Ravi Kumar)

This is to certify that the above statement made by the candidate is correct to the best of my/our knowledge.

Signature of the Supervisor with date
(Dr. Shaikh M. Mobin)

Mr. Ravi Kumar has successfully given his/her M.Sc. Oral Examination held on **……..**

Signature of the Thesis Supervisor
Date:

Convener, DPGC
Date:

Signature of the PSPC Member
Date:

Signature of the PSPC Member
Date:

ACKNOWLEDGEMENTS

With deep regards and profound respect, I avail this opportunity to express my deep sense of gratitude and indebtedness to Dr. Shaikh M. Mobin for introducing the present project topic and for his inspiring guidance, constructive criticism and valuable suggestion throughout the project work. I gratefully acknowledge his constant encouragement and help in different ways to complete this project successfully. I would also like to extend my gratitude to Dr. Rajneesh Misra and Dr. Santosh K. Vishvakarma for their valuable suggestions and guidance.

I extend my profound thanks to my group members, Dr. Dhirender Kumar Rai, Dr. Archana Chaudhary, Dr. Ramprakash Venkatesan, Mrs. Veenu Mishra, Mr. Anoop Kumar Saini, Mr. Akbar Mohammad, Mr. Ajeet Singh, Mr. Vinay Sharma Mr. Mohit Saraf and Ms. Kshipra Kapoor for their generous co-operation and help to make my work successful.

I would like to record my thanks to Mr. Bishnubasu Giri, Mr. Sahidul Mondal and Mr. Ankan Biswas, Mr. Rupenayan borah, Mr. Md. Balal, Mr. Rohit Gupta, Mr. Ashish Sehrawat, Mr. Sourabh Solanki, Mr. Jigar Choudhary and Uttiya Sarkar.

I am thankful to Ms. Sarita Batra, Mr. Kinney Pandey, Mr. Ghanshyam Bhavsar and Mr. Manish Kushwaha for their technical help and support. I need to express my deepest love and gratitude to my lovable father Mr. Sanjay Gupta and to my lovable mother Mrs. Laxmi for their uncond- itional love with full support, unending encouragement and patience during this tenure.

Ravi Kumar

DEDICATED TO MY BELOVED PARENTS

ABSTRACT

The work described in this thesis concerns the synthesis of aroylhydrazone ligands. The aroylhydrazone ligands *b*is[4-phenylbenylidene]pyridine-2,6-dicarbohydrazide (**L1)**, *bis*[4-(4-pyridyl)benylidene]pyridine-2,6-dicarbo-hydrazide (**L2)**, *bis*[3-cyanobenylidene]pyridine-2,6-dicarbohydrazide (**L3)** and *bis*[3-cyanobenylidene]pyridine-2,6-dicarbohydrazide (**L4)** were synthesized by condensation reactions of pyridine-2,6-dicarbohydrazide with 4-phenyl-benzaldehyde, 4-(4-pyridyl)benzaldehyde, 3-cyanobenzaldehyde and 2,3,4-trihydroxybenzaldehyde, respectively. These ligands have been characterized by Mass spectrometry, Infrared spectroscopy, and NMR spectroscopy. The molecular structures of ligands (**L1-L4**) and their three dimensional supramolecular interactions have been investigated by single crystal X-ray diffraction analysis. It was found that all studied hydrazones adopt the E configuration around the imino N=C group in the solid state. The association modes in the studied crystals are dominated by strong hydrogen bonds of the N−H…O type involving the amide group as a proton donor.

TABLE OF CONTENTS

LIST OF FIGURES

LIST OF TABLES

NOMENCLATURE

θ	Angle
λ	Wavelength
α	Alfa
β	Beta
γ	Gamma
Å	Angstrom
δ	delta
mm	Millimeter
π	Pi
mg	Milligram
d	Density
m	meter
K	Kelvin
μ	Dipole moment
v	Volume

ACRONYMS

br	broad
$CDCl_3$	Chloroform-d
d	Doublet
DMF	Dimethyl Formamide
DMSO-d_6	Dimethylsuphoxide-d
ESI-MS	Electrospray Ionization Mass Spectrometry
EtOH	Ethanol
FTIR	Fourier Transform Infrared Spectroscopy
H_2O	Water
m	Multiplet
MeOH	Methanol
NMR	Nuclear Magnetic Resonance
s	Singlet
t	Triplete

Chapter 1

Introduction

1.1 General Introduction and Literature Background

Over the past few decades the chemistry of aroyl hydrazones has been the subject of much interest. Many papers and reviews concerning the use of hydrazones derivatives in organic [1-3], organometallic [4, 5], analytical chemistry [6, 7] and medicinal chemistry [8] have been published for their potential applications in these areas. Figure 1.1 shows the structural and functional diversity of hydrazone moiety [9]. These structural and electronic features determine the physicochemical properties and biological activities of aroyl hydrazone to a large extent.

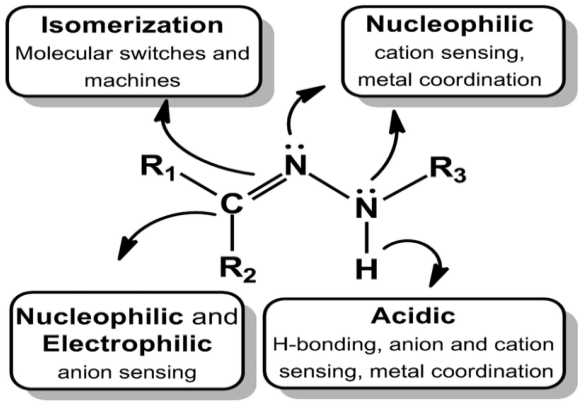

Figure 1.1. *The structural and functional diversity of the hydrazone group*

1.2 Aroyl Hydrazones

Hydrazones belong to a class of azomethines, having a —C=N—N— moiety, rendering it to be an interesting ligand in coordination chemistry. They are differentiated by other members of this family by the presence of two interlinked nitrogen formed by the condensation reaction between a hydrazide with a carbonyl compound. Presence of a —C=O group in the hydrazide part increases the electron delocalization and denticity of the hydrazone and the resulting compound is known as an aroyl hydrazone. Their purification can be accomplished by recrystallization and they are stable at ambient temperature.

Figure 1.2 represents the general formula of a hydrazone and an aroyl hydrazone.

Hydrazone **Aroylhydrazone**

Figure 1.2. *General formula for a substituted hydrazone and aroyl hydrazone.*

Aroyl hydrazones allow additional donor sites to be introduced (*via* R, R1 and R2, Figure l.2.) in order to increase the denticity of the resulting ligands. In an aroyl hydrazone the basic coordination sites are carbonyl oxygen and the azomethine nitrogen. It is interesting to note that aroyl hydrazones can potentially form amido/iminol tautomers as indicated in Figure 1.3.

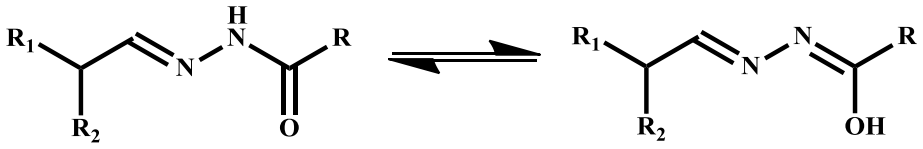

Amido form **Iminol form**

Figure 1.3. *Tautomerism in aroyl hydrazone.*

1.3 Applications of Aroyl Hydrazones

The aroyl hydrazone moiety is ubiquitous in various fields ranging from organic synthesis, medicinal chemistry and nonlinear optics to supramolecular chemistry.

1.3.1 Aroyl Hydrazone in Non Linear Optics (NLO)

Aroyl hydrazones have been revealed as an important class of organic crystalline materials. It is reported that hydrazones can act as a π bridge for π electron delocalization across the donor-acceptor links which is important for showing nonlinear optical [NLO] activities. Due to this aroyl hydrazones and their metal complexes show huge potential in optoelectronic devices. Naseema *et al*. found the influence of donor/acceptor groups on the nonlinear optical properties of some aroyl hydrazone derivatives [10]. Cariati *et al.* investigated the second order nonlinear optical properties of copper and palladium complexes of N-

salicylidene-N′-aroyl hydrazones and found that these complexes have considerable NLO activity [11].

1.3.2 Aroyl Hydrazone in Medicinal Chemistry

Aroyl hydrazones possessing an azomethines and amide proton -CO-NH–N=CH-, constitute an important class of compounds for new drug development. Aroyl hydrazone has been reported to possess remarkable antibacterial, antifungal, anticancer, antioxidant, anti-inflammatory and anti-malarial activities [12, 13]. Walcourt *et al*. synthesized a series of aroyl hydrazone derivatives with significant antimalarial activity [14].

1.3.3 Aroyl Hydrazone in Analytical Chemistry

Aroyl hydrazones are extensively used as analytical reagents because they react with metal ions and form colored precipitate or solutions. It is possible to implicate them in analytical chemistry for ultra trace determination of metal ions, development of sensors and as acid-base indicators based on such complexes. In 2006, Tong *et al.* investigated an ‘‘off-on’’ fluorescent chemosensor for Cu^{2+} based on a rhodamine B-based aroyl hydrazone [15]. Krishna *et al.* have reported a simple, sensitive and selective spectrophotometric method for the determination of Cd(II) in biological materials (Cigarette tobacco, Radish flesh and Cabbage) and in alloy samples using cinnamaldehyde-4-hydroxybenzoyl hydrazone [16].

1.3.4 Aroyl Hydrazone in Catalytic Applications

Aroyl hydrazones and their complexes have attracted considerable attention due to their high synthetic potential in catalysis. The use of nitrogen containing ligands leads to an increased catalytic activity [17]. Aroyl hydrazone complexes are good candidates for catalytic oxidation because of their ability to resist oxidation. Monas *et al.* have reported catalytic potential of Cu(II) complexes of aroyl hydrazone towards mild hydrocarboxylation of alkanes [18]. Monas *et. al.* have also reported catalytic activity of Mn(II) dinuclear complexes towards microwave assisted oxidation of alcohols [19]. Mizar *et al.* demonstrated that copper(II) complexes of aroyl hydrazones derived from β-diketones can be used as efficient and selective catalysts for the peroxidative oxidation of cyclohexene to cyclohex-2-enol and cyclohex-2-enone under mild conditions [20]. Dipali *et.*

al. investigated the catalytic potential for epoxidation of alkenes under phase transfer conditions [21].

1.4 Organization of the Thesis

The aim of this project was to synthesize different structural motifs of aroyl hydrazone. This was to be achieved by synthesizing various pyridine-2,6-dicarbohydrazide based hydrazone moieties and their subsequent complexation with suitable metal ions.

Chapter 2: This chapter includes materials, techniques and experimental procedure which were used to synthesize aroyl hydrazone.

Chapter 3: In this chapter, we have discussed about the results that was obtained during synthesis of these ligand.

Chapter 4: In this chapter, we have concluded all the results of our work and their future aspects.

Chapter 2

Experimental Section

2.1 General Information and Physical Measurements

All chemicals of reagent grade quality were purchased from commercial available sources and were used without further purification. The pyridine-2,6-dicarbohydrazide was synthesized according to the reported method [22]. Melting point of the ligands were determined using aluminium block accepts three capillary tubes and mercury thermometer. The ^{1}H and ^{13}C NMR spectra were recorded on a JNM-ECS400 (JEOL) instrument operated at 400 MHz for ^{1}H NMR and 100 MHz for ^{13}C NMR. The chemical shifts are reported as delta values (ppm) relative to TMS. IR spectra were recorded on a Bruker Tensor 27 spectrometer for the compounds in the solid state as KBr discs or as neat samples. Mass spectra of aroyl hydrazones were recorded on Bruker micrOTOF-Q II by positive and negative mode electrospray ionizations.

2.2 X-ray Crystallography

Single crystal X-ray structural studies of **(L1-L4)** were performed on a CCD Agilent technology supernova diffractometer equipped with a low-temprature attachment. Data were collected at 150(2) K using graphite-monochromoated Mo Kα radiation (λ_{α} = 0.71073 Å). The strategy for the Data collection was evaluated by using the CrysAlisPro CCD software. The data were collected by the standard 'phi-omega scan techniques, and were scaled and reduced using CrysAlisPro RED software. The structures were solved by direct methods using SHELXS-97 and refined by full matrix least squares with SHELXL-97, refining on F^2. The positions of all the atoms were obtained by direct methods. All the H-bonding inter-actions, mean plane analyses, and molecular drawings were obtained using the program Diamond (version 3.1).

2.3 Synthesis of Aroyl Hydrazone Ligands

2.3.1 Synthesis of *bis*[4-phenylbenzylidene]pyridine-2,6-dicarbo-hydrazide (L1)

A solution of pyridine-2,6-dicarbohydrazide (0.195 g, 1 mmol) and 4-phenylbenzaldehyde (0.364 g, 2.0 mmol) in 50 ml of methanol was refluxed for 10 h. Upon completion of reaction, white colored precipitate was obtained. The precipitate was filtered off, washed with methanol and dried in vacuum oven. This precipate was dissolved in 1:1 (v/v) methanol and acetone mixture and left for crystallization. On slow evaporation of the solvent, white colored crystal of **L1** was obtained after 5-6 days in 90% yield. Melting Point: 280-282 °C; Anal. Calcd for $C_{33}H_{25}N_5O_2$: C, 75.70; H, 4.81; N, 13.38. Found: C, 75.12; H, 4.80; N, 13.55; HRMS (ES^+) calcd for $[M+H]^+$ $C_{33}H_{25}N_5O_2$ 524.58, found 524.22; IR (KBr, cm^{-1}): 3448, 3254, 3227, 3028, 2924, 2362, 2343, 1700, 1660, 1606, 1589, 1534, 1485; ^1H NMR δ_H (400 MHz, DMSO-d_6) 12.39 (s, 2H), 8.83 (s, 2H), , 8.38 (d, *J*=8 Hz, 2H), 8.30 (t, *J*=8 Hz, 1H), 7.93 (d, *J*=8 Hz, 4H), 7.83 (d, *J*=8 Hz, 4H), 7.75 (d, *J*=8 Hz, 4H), 7.50 (t, *J*=8 Hz, 4H), 7.40 (t, *J*=8 Hz, 2H); ^{13}C NMR δ_C (100 MHz, DMSO-d_6) 159.45 (C=O), 149.70 (Py-C), 148.27 (C=N), 141.95 (Ar-C), 139.97 (Ar-C), 139.28 (Py-C), 133.22 (Ar-C), 129.03 (Ar-C), 127.92 (Ar-C), 127.12 (Ar-C), 126.71 (Ar-C), 125.50 (Py-C).

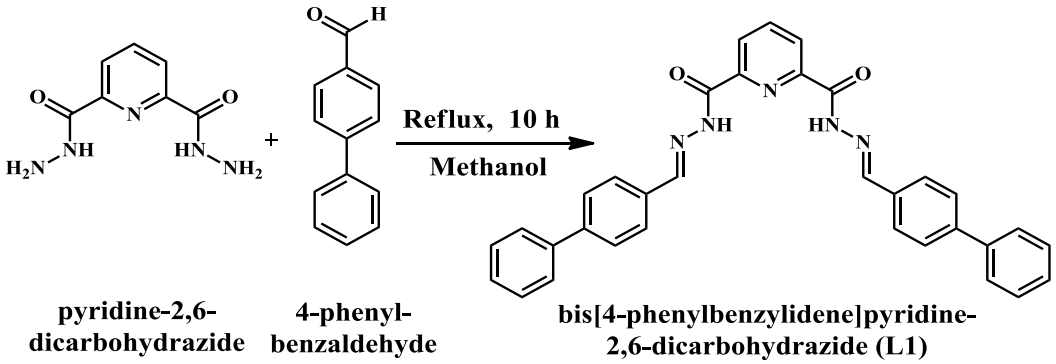

Figure 2.1. *Schematic representation for the synthesis of bis[4-phenyl-benylidene]pyridine-2,6-dicarbohydrazide* ***(L1)*****.**

2.3.2 Synthesis of *bis*[4-(4-pyridyl)benylidene]pyridine-2,6-dicarbo hydrazide (L2)

A solution of pyridine-2,6-dicarbohydrazide (0.195 g, 1 mmol) and 4-(4-pyridyl)benzaldehyde (0.366 g, 2.0 mmol) in 50 ml of methanol was refluxed for 15 h. Upon completion of reaction, light yellow color precipitate was obtained. The precipitate was filtered off, washed with methanol and dried in vacuum oven.

This precipitate was dissolved in 1:1 (v/v) ethanol and chloroform mixture and left for crystallization. On slow evaporation of the solvent, white colored crystal of **L2** was obtained after 2-3 days in 88% yield. Melting Point: 326-328 °C; Anal. Calcd for $C_{31}H_{23}N_7O_2$: C, 70.84; H, 4.41; N, 18.66. Found: C, 70.82; H, 4.42; N, 18.67; HRMS (ES^+) calcd for $[M+H]^+$ $C_{31}H_{23}N_7O_2$ 526.19, found 526.20; IR (KBr, cm^{-1}): 3440, 3195, 3033, 2360, 2341, 1674, 1604, 1539; ^1H NMR δ_H (400 MHz, DMSO-d_6) 12.44 (s, 2H), 8.85 (s, 2H), 8.67 (d, *J*=8 Hz, 4H), 8.38 (d, *J*=8 Hz, 2H) , 8.30 (t, *J*=8 Hz, 1H), 7.97 (t, J=8 Hz, 8H), 7.78 (d, *J*=4 Hz, 4H); ^{13}C NMR δ_C (100 MHz, DMSO-d_6) 159.72 (C=O), 150.34 (Py1-C), 149.30 (Py2-C), 148.39 (C=N), 146.15 (Py2-C), 138.72 (Py1-C), 135.09 (Ar-C), 129.64 (Ar-C), 128.00 (Ar-C), 127.40 (Ar-C), 125.61 (Py1-C), 121.16 (Py2-C).

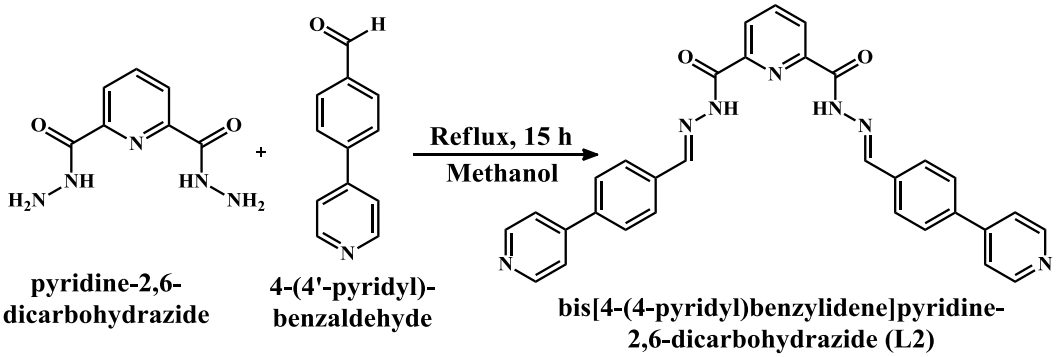

Figure 2.2. *Schematic representation for the synthesis of bis[4-(4-pyridyl)-benzylidene]pyridine-2,6-dicarbohydrazide* ***(L2).***

2.3.3 Synthesis of *bis*[3-cyanobenylidene]pyridine-2,6-dicarbohydrazide (L3)

A solution of pyridine-2,6-dicarbohydrazide (0.195 g, 1 mmol) and 3-cyanobenzaldehyde (0.263 g, 2.0 mmol) in 50 ml of methanol was refluxed for 24 h. Upon completion of reaction, white colored precipitate was obtained. The precipitate was filtered off, washed with methanol and dried in vacuum oven. This precipitate was dissolved in DMF. On slow evaporation of the solvent, white colored crystal of **L3** was obtained after one month in 76% yield. Melting Point: 330-332 °C; Anal. Calcd for $C_{23}H_{15}N_7O_2$: C, 65.55; H, 3.59; N, 23.27. Found: C, 65.59; H, 3.61; N, 23.30; HRMS (ES^+) calcd for $[M+H]^+$ $C_{23}H_{15}N_7O_2$ 422.13, found 422.14; IR (KBr, cm^{-1}): 3490, 3418, 3200, 2360, 2341, 2228, 1686, 1651,

1540, 1364, 1169, 685; ^{1}H NMR δ_H (400 MHz, DMSO-d_6) 12.50 (s, 2H), 8.81 (s, 2H), 8.39(d, *J*=8 Hz, 2H), 8.30(t, *J*=8 Hz, 1H), 8.17 (t, *J*=8 Hz, 4H), 7.94 (d, *J*=8 Hz, 2H), 7.72(t, *J*=8 Hz, 2H); ^{13}C NMR δ_C (100 MHz, DMSO-d_6) 159.67 (C=O), 148.06 (Py-C), 147.74 (C=N), 140.12 (Py-C), 135.44 (Ar-C), 133.64 (Ar-C), 131.15 (Ar-C), 130.90 (Ar-C), 130.26 (Ar-C), 125.75 (Py-C), 118.33 (CN), 112.16 (Ar-C).

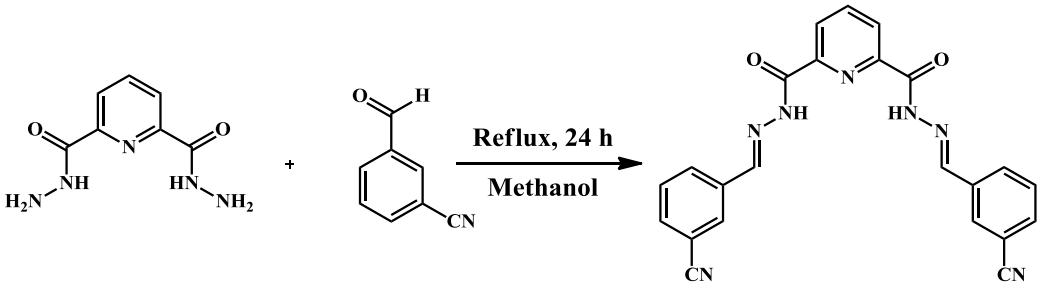

pyridine-2,6-dicarbohydrazide **3-cyanobenzaldehyde** **bis[3-cyanobenzylidene]pyridine-2,6-dicarbohydrazide (L3)**

Figure 2.3. *Schematic representation for the synthesis of bis[3-cyanobenylidene]-pyridine-2,6-dicarbohydrazide* ***(L3).***

2.3.4 Synthesis of *bis*[2,3,4-trihydroxybenzylidene]pyridine-2,6-dicarbo hydrazide(L4)

A solution of pyridine-2,6-dicarbohydrazide (0.195 g, 1 mmol) and 2,3,4-dihydroxybenzaldehyde (0.308 g, 2.0 mmol) in 50 ml of methanol was refluxed for 12 h. Upon completion of reaction, yellow colored precipitate was obtained. The precipitate was filtered off, washed with methanol and dried in vacuum oven. This precipitate was dissolved in 1:1 (v/v) water and acetone mixture and left for crystallization. On slow evaporation of the solvent, yellow colored crystal of **L4** was obtained after 11 days in 84% yield. Melting Point: >350°C; Anal. Calcd for $C_{21}H_{17}N_5O_8$: C, 53.96; H, 3.67; N, 14.98. Found: C, 54.01; H, 3.61; N, 14.96; HRMS (ES^+) calcd for $[M+H]^+$ $C_{21}H_{17}N_5O_8$ 468.11, found 422.10; IR (KBr, cm^{-1}): 3442, 2925, 2854, 2360, 2341, 1638, 1588, 1512, 1383, 1341, 1265; ^{1}H NMR δ_H (400 MHz, DMSO-d_6) 12.30 (s, 2H), 11.27 (s, 2H), 9.62 (s, 2H), 8.71 (s, 2H), 8.57 (s, 2H) , 8.34(d, *J*=4 Hz, 2H) , 8.27 (t, *J*=8 Hz, 1H), 6.91 (d, *J*=8 Hz, 2H), 6.44(d, *J*=8 Hz, 2H) ; ^{13}C NMR δ_C (100 MHz, DMSO-d_6) 159.15 (C=O), 152.00 (Ar-C), 149.26 (Ar-C), s148.12 (Py-C), 147.78 (C=N), 140.15 (Py-C), 132.90

(Ar-C), 125.54 (Py-C), 121.29 (Ar-C), 111.00 (Ar-C), 108.03 (Ar-C).

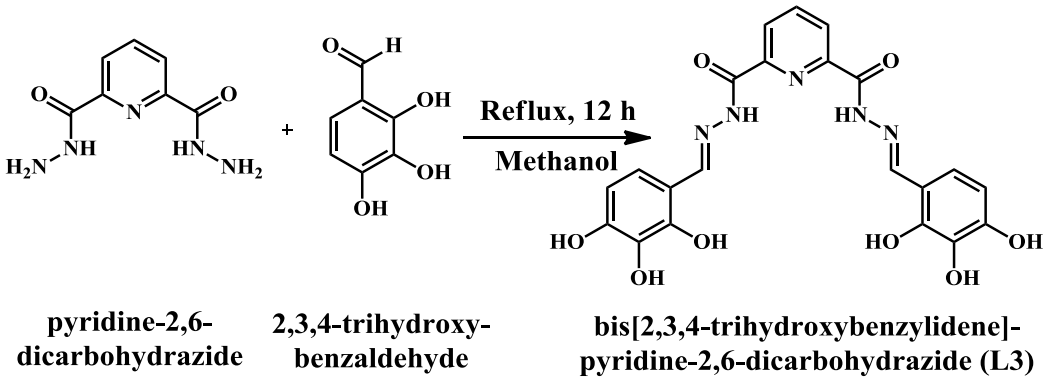

Figure 2.4. *Schematic representation for the synthesis of bis[2,3,4-trihydroxy-benzylidene]pyridine-2,6-dicarsbohydrazide* ***(L4).***

Chapter 3

Results and discussion

3. 1 Characterization of L1

3.1.1 Mass Spectrometry

ESI-MS data supports the formation of **L1** with molecular ion peaks at m/z 546.21 and 524.22 which correspond to the $[M+Na]^+$ and $[M+H]^+$, respectively.

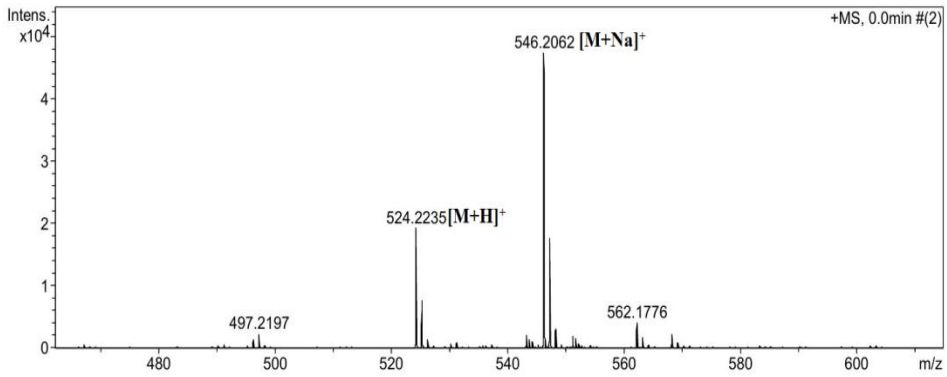

Figure 3.1. *ESI-MS spectrum of* ***L1.***

3.1.2 Infrared Spectroscopy

In the IR spectrum of **L1** an intense band was observed at 1660 cm^{-1} attributed to *ν*(-C=N) of azomethines. Another intense band at 1699 cm^{-1} corresponds to the *ν*(-C=O), of the carbonyl group of the amide bond. An intense band at 3230 cm^{-1} is due to *ν*(–NH-), of amide bond and band at 1533 cm^{-1} corresponds to the C-H stretching in H-C=N group present in **L1**. Appearance of these bands suggests the presence of amide and azomethines functional group in **L1.** [Fig. 3.2]

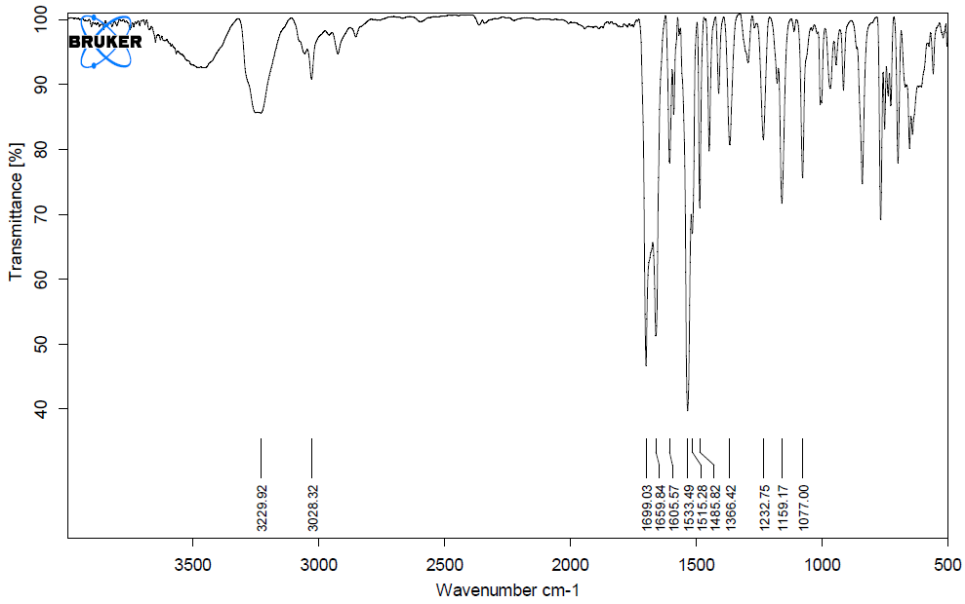

Figure 3.2. *IR spectrum of* ***L1.***

3.1.3 NMR Spectroscopy

NMR spectra of **L1** were recorded in DMSO-d_6 using TMS as an internal standard. It is known that symmetric C and H atoms in the compounds have the same chemical environment of the atoms. Chemical shift values of **L1** are in reasonable agreement with literature data for the similar compounds [23, 24]. In NMR spectrum, aromatic carbon peaks were shown at 110–160 ppm and aromatic proton peaks were observed at about 6.8–8 ppm.

The ^{13}C NMR spectrum for the **L1** is given below in Figure 3.3. A peak near 159.45 ppm corresponds to carbonyl carbon in compound, a peak at 149.70 ppm is attributed to pyridine ring carbon attached to carbonyl group and a peak near 148.27 ppm corresponds to the imine carbon. All other peaks represent the aromatic carbons.

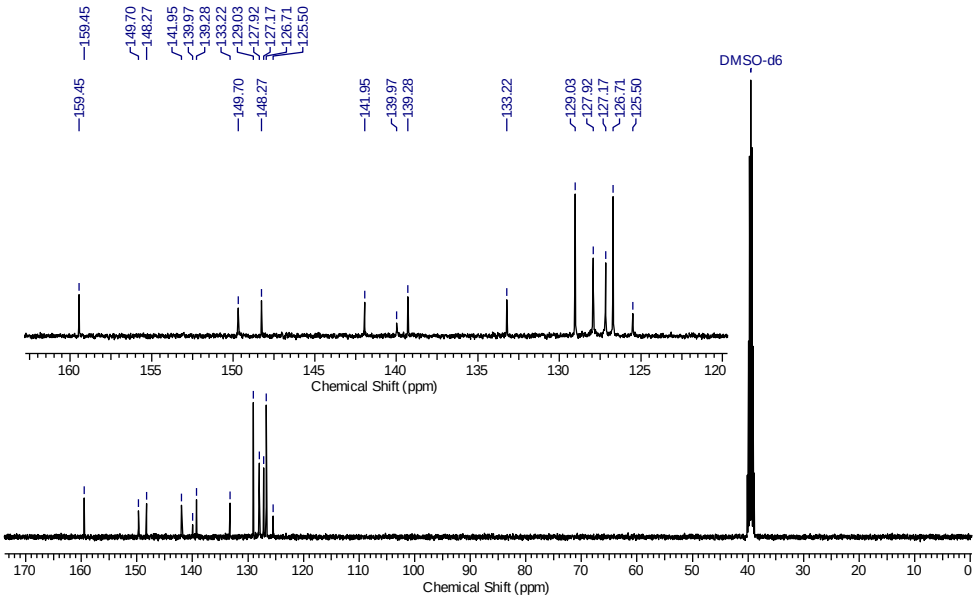

Figure 3.3. *^{13}C NMR spectrum of **L1** in DMSO-d_6.*

The ^{1}H NMR spectrum for the L1 is given in Figure 3.4, peaks in the region 7.39 to 8.39 ppm were assigned to the proton of aromatic rings. The signals near 12.39 and 8.83 were assigned to the proton of amide –CONH- and imine –CH=N group, respectively.

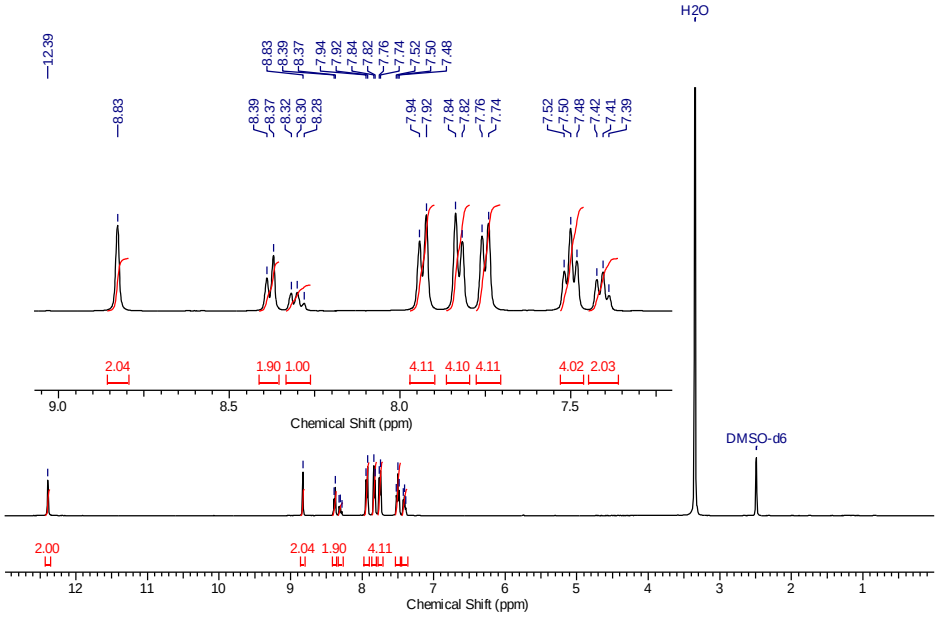

Figure 3.4. *^{1}H NMR spectrum of **L1** in DMSO-d_6.*

3. 1.4 Crystal Structure of L1

The white needle shaped crystal of **L1** suitable for X- ray diffraction analysis was obtained by crystallization from a mixture of methanol and acetone (1:1 v/v). A single crystal with approximate dimensions of 0.230 x 0.170 x 0.130 mm^3 was selected for collecting the data. The molecular structure of the compound with the atom numbering scheme is given in Figure 3.5. The crystallographic data and structure refinement parameters of the compound are given in Table A.1.

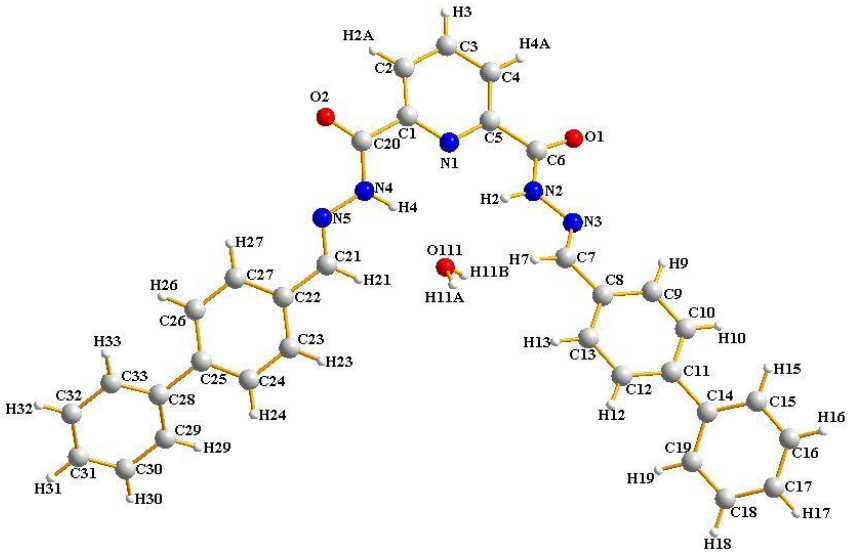

Figure 3.5. *Molecular structure of* ***L1*** *and water molecule along with the atom numbering scheme.*

The aroyl hydrazone, **L1** is crystallizes in a triclinic crystal space group *P*ī. The one molecule of **L1** contains a lattice water molecule [Figure 3.5]. In this case the empirical formula of **L1** $C_{33}H_{27}N_5O_3$ can be written as $C_{33}H_{25}N_5O_2.H_2O$.

Figure 3.6 shows the 2-D structure of **L1** with the intermolecular interaction. This 2-D structure formed due to the CH… π interactions of one molecule of **L1** to other molecule of **L1**. The distance of these interactions are 3.579 Å between C(23)-H23...D(1) and 3.759 Å between C(30)-H(30)…D(2).

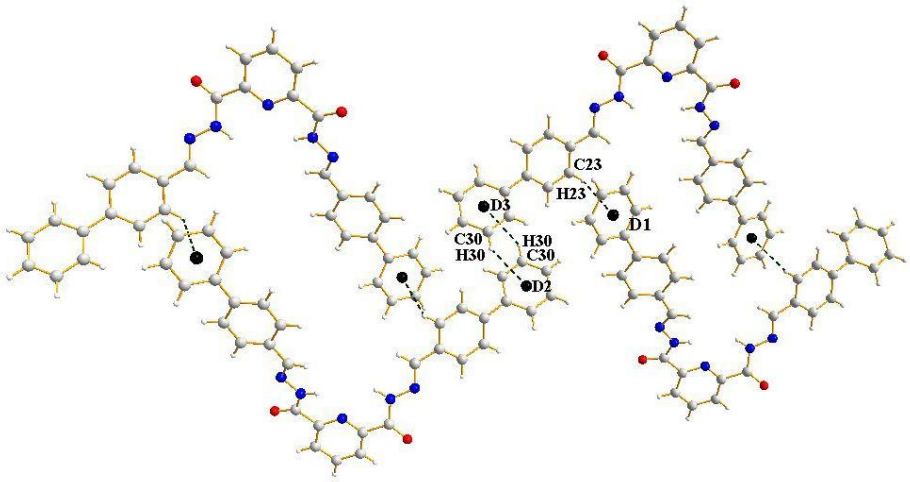

Figure 3.6. *2-D structure of* ***L1*** *due to intermolecular interaction.*

One water molecule is linked to three ligand units *via* H-bonding inter- actions. Molecule **1** is involved in H-bonding *via* O(111)- H(11B)…N(3) (2.216 Å), and O(111)- H(11B)...O(1) (2.472 Å). Molecule **2** interacts *via* N(2)-H(2)…O(111) (2.544 Å), N(4)-H(4)…O(111) (2.192 Å) and C(21)- H(21)...O(111) (2.417 Å). Molecule **3** makes only one interaction with water molecule *i.e.* O(111)-H(11A)...O(2) (2.226 Å). These interactions of water molecule formed 3-D structure of **L1**.

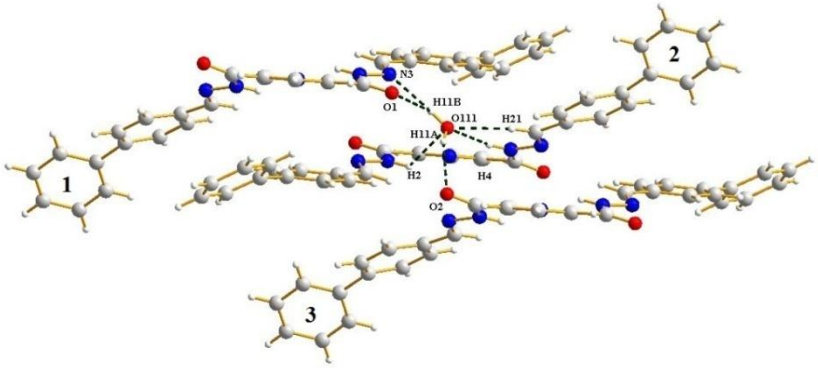

Figure 3.7. *Interactions of water molecule with* ***L1****.*

Figure 3.8 shows the packing diagram of the compound **L1** along *b* axis. The packing of molecules in the respective manner in the unit cell is resulted by the CH…π and H-bonding interaction.

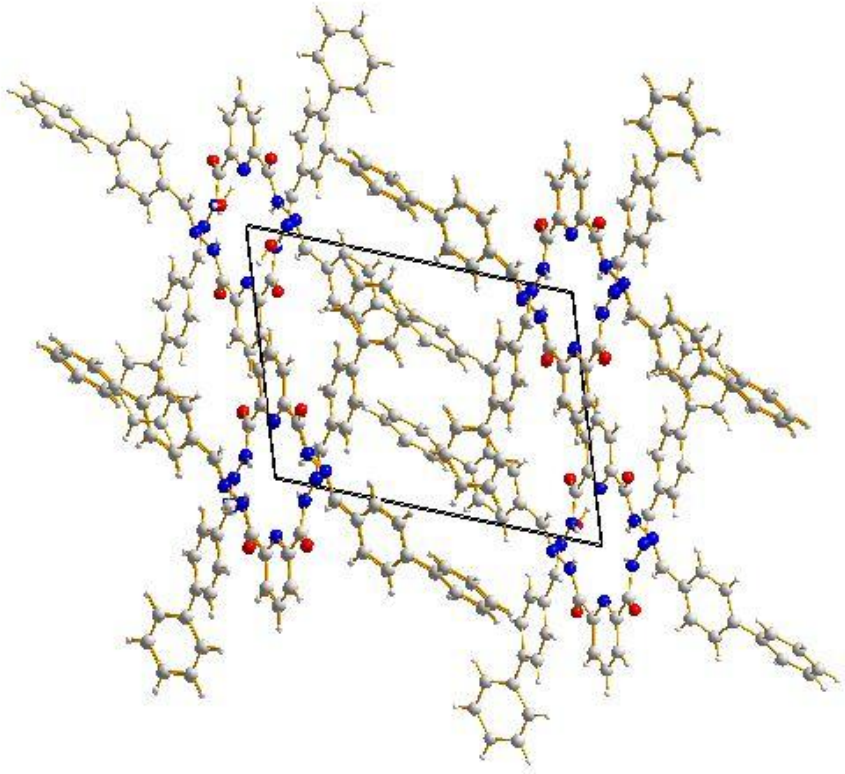

Figure 3.8. *Packing diagram of* ***L1*** *along b axis.*

3.2 Characterization of L2

3.2.1 Mass Spectrometry

ESI-MS data supports the formation of **L2** with molecular ion peaks at m/z 548.20 and 526.20 which correspond to the $[M+Na]^+$ and $[M+H]^+$, respectively.

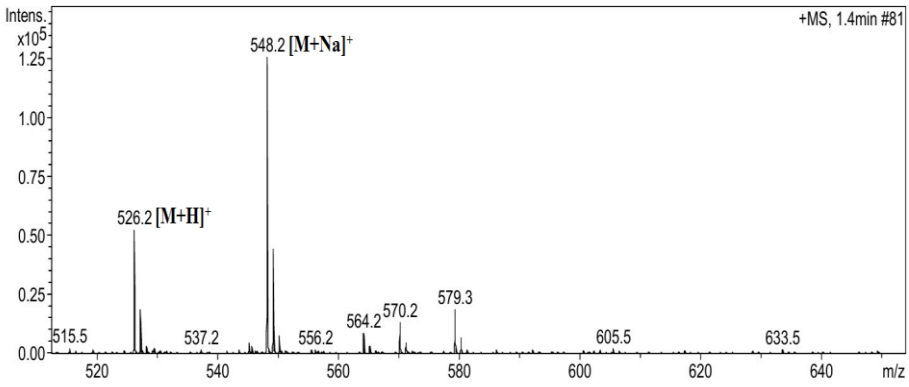

Figure 3.9. *ESI-MS spectrum of* ***L2.***

3.2.2 Infrared Spectroscopy

In the IR spectrum of **L2** an intense band was observed at 1596 cm^{-1} attributed to

v(-C=N), of azomethines. Another intense band at 1683 cm^{-1} corresponds to the *v* (-C=O), of the carbonyl group of the amide bond. An band at 3238 cm^{-1} is due to the *v*(–NH-) and intense band at 1539 cm^{-1} corresponds to the C-H stretching in H-C=N group in **L2**. Appearance of these bands suggests the presence of amide and azomethines functional group in **L2** [Fig. 3.10]

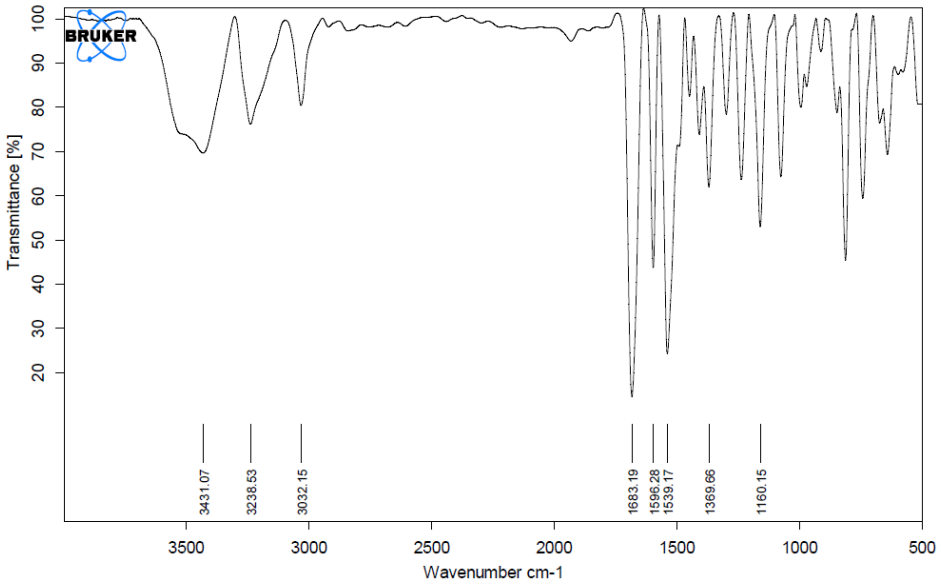

Figure 3.10. *IR spectrum of* ***L2.***

3.2.3 NMR Spectroscopy

NMR spectra of **L2** were recorded in DMSO-d_6 using TMS as an internal standard. A ^{13}C NMR spectrum for the **L2** is given below in Figure 3.11. The spectrum shows twelve different types of carbons in **L2** molecule. A peak near 159.72 ppm corresponds to carbonyl carbon in compound, peak at 150.36 ppm is attributed to pyridine ring carbon attached to carbonyl group and peak near 148.39 ppm corresponds to the imine carbon. All other peaks show aromatic carbons.

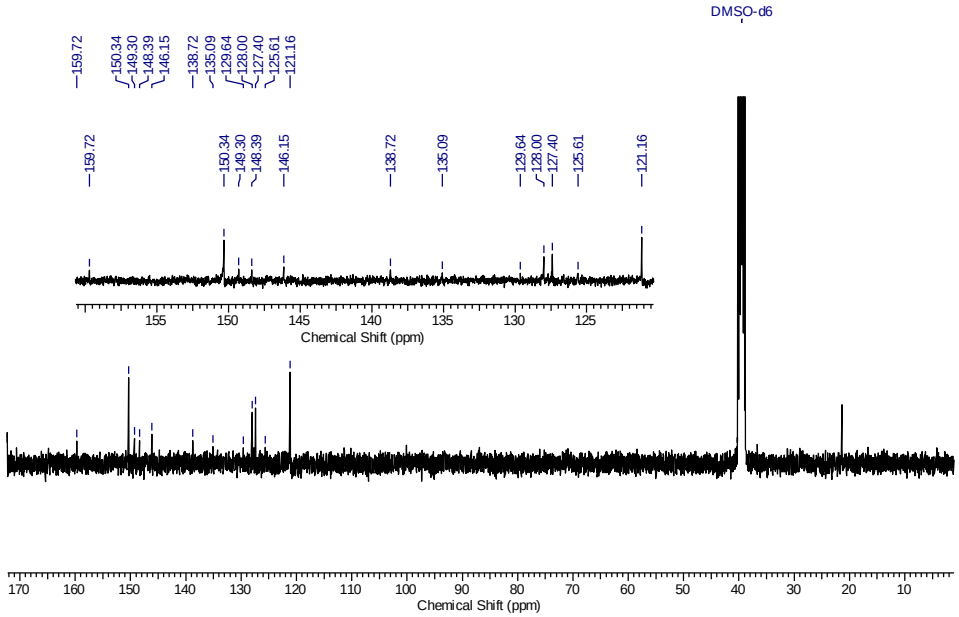

Figure 3.11. *^{13}C NMR spectrum of **L2** in DMSO-d_6.*

The ^{1}H NMR spectrum for the **L2** is given in Figure 3.12, peaks in the region 7.39 to 8.68 ppm were assigned to the proton of aromatic rings. The peaks near 12.44 and 8.85 were assigned to the proton of amide –CONH- and imine –CH=N groups, respectively.

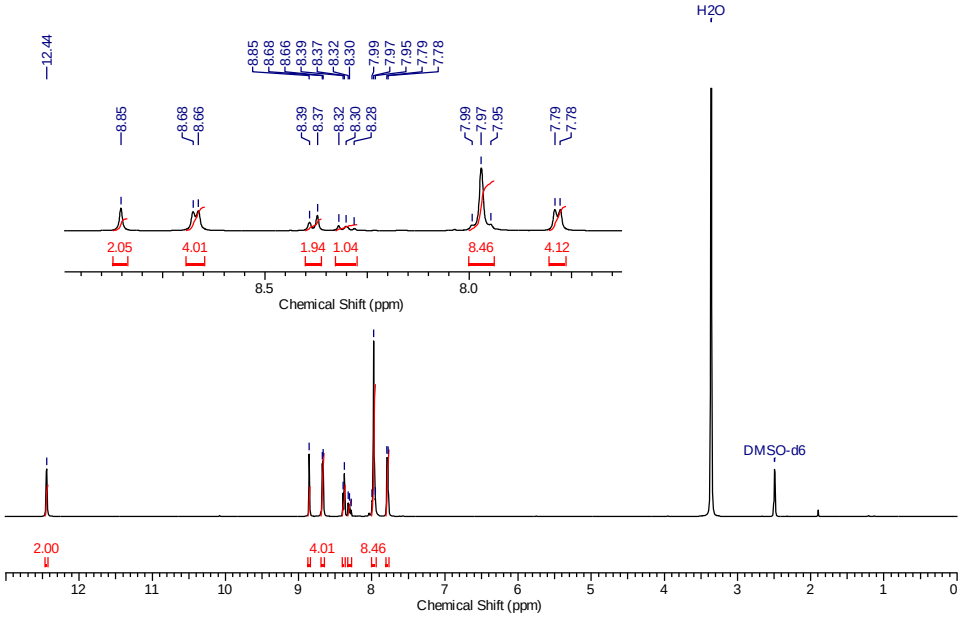

Figure 3.12. *^{1}H NMR spectrum of **L2** in DMSO-d_6.*

3.2.4 Crystal Structure of L2

The light yellow color shiny needle shaped crystal of **L2** suitable for X- ray diffraction analysis was obtained by crystallization from a mixture of chloroform and ethanol (1:1 v/v). A single crystal with approximate dimensions of 0.210 x 0.170 x 0.130 mm^3 was selected for data collection. The molecular structure of the compound with the atom numbering scheme is given in Figure 3.13. The crystallographic data and structure refinement parameters of the compound are given in Table A.1.

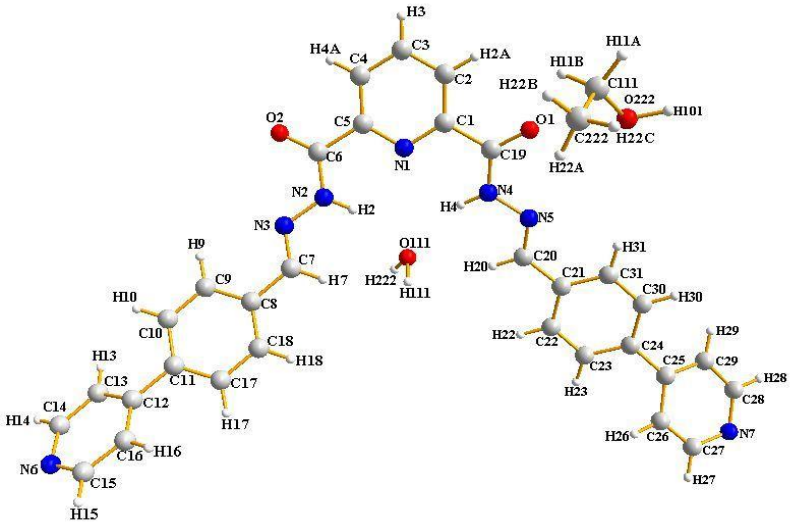

Figure 3.13. *Molecular structure of **L2** with lattice water and ethanol molecule along with the atom numbering scheme.*

The aroyl hydrazone, **L2** is crystallized into a monoclinic space group *P* 21/*c*. The one molecule of **L2** containing a lattice water and an ethanol molecule is shown in Figure 3.13. In this case the empirical formula of **L1** $C_{33}H_{31}N_7O_4$ can be written as $C_{31}H_{23}N_7O_2.H_2O.C_2H_6O$.

Figure 3.14 shows the 2-D structure of **L2** with intermolecular interaction. This 2-D structure formed due to two non-conventional H-bonding through C(29)-H(29)…N(7) (2.717 Å) and C(26)-H(26)...O(1) (2.502 Å) and one CH… π interaction between C(2)-H(2A)…D(1) (3.672 Å).

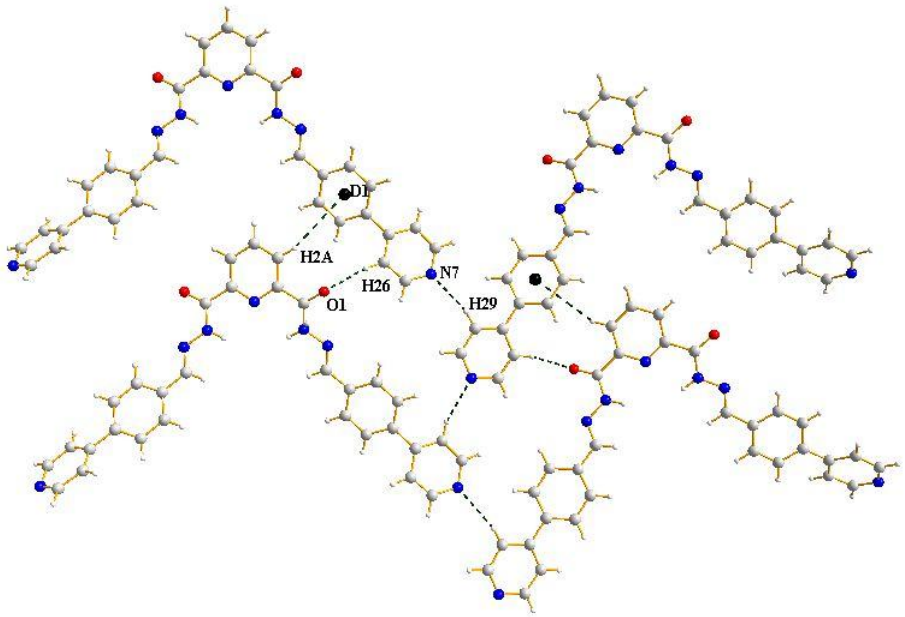

Figure 3.14. *2-D structure of* ***L2*** *due to intermolecular interactions.*

One water molecule is linked with two ligand units and one ethanol *via* H-bonding interactions. Molecule **1** is involved in H-bonding with water hydrogen and ligand carbonyl group *via* O(111)-H(222)…C(19)-O(1) (2.086 Å). Molecule **2** interacts with water oxygen *via* N(2)-H(2)...O(111) (2.263 Å), N(4)-H(4)…O(111) (2.214 Å), C(7)-H(7)...O(111) (2.655 Å) and C(20)-H(20)...O(111) (2.502 Å). One strong hydrogen bond between hydrogen of water and oxygen of ethanol molecule is observed *via* O(111)-H(111)...O(222) (1.943). Molecule **3** makes three interaction with ethanol molecule. These interactions are as follows C(9)-H(9)…O(222) (2.570 Å), O(222)-H(101)...O(2) (1.883 Å), O(222)-H(101)…N(3) (2.487 Å). These interactions of water and ethanol molecules formed 3-D structure of **L2**.

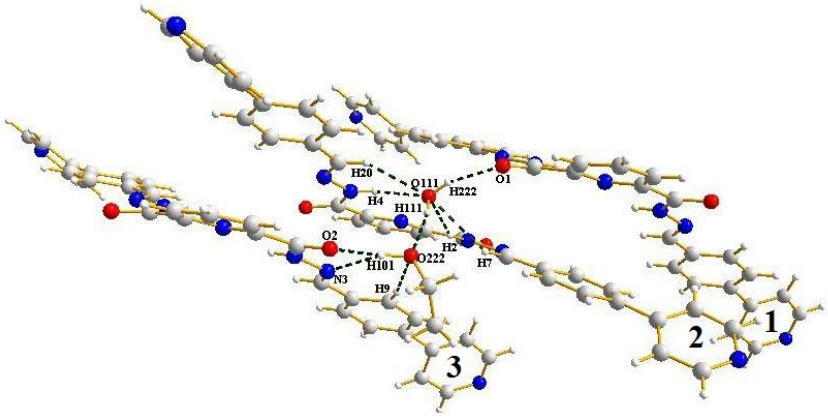

Figure 3.15. *Interactions of water molecule and ethanol molecule with* ***L2****.*

Figure 3.16 shows the packing diagram of the compound **L2** along *b* axis. The packing of molecules in the respective manner in the unit cell is resulted by CH…π and H-bonding interactions.

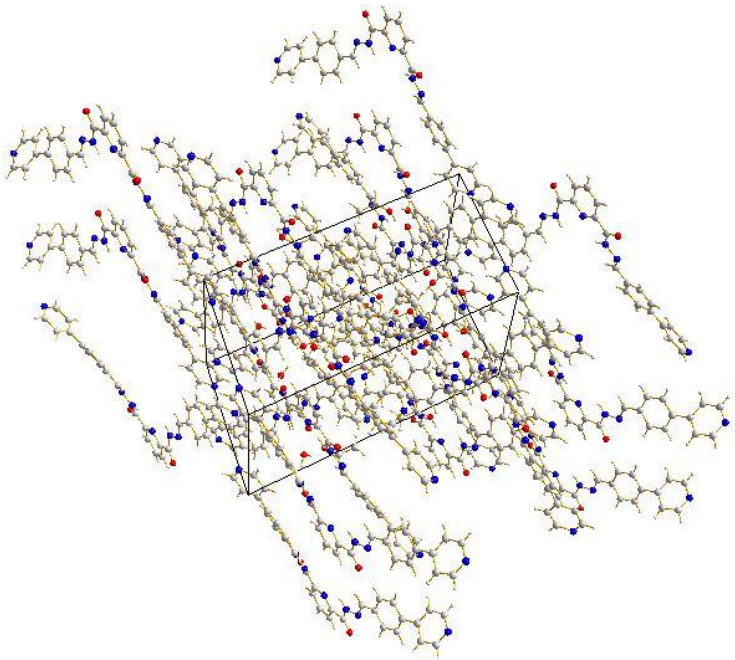

Figure 3.16. *Packing diagram of* ***L2*** *along b axis.*

3. 3 Characterization of L3

3.3.1 Mass Spectrometry

ESI-MS data supports the formation of **L3** with molecular ion peaks at m/z 444.12 and 422.14 corresponding to the $[M+Na]^+$ and $[M+H]^+$, respectively.

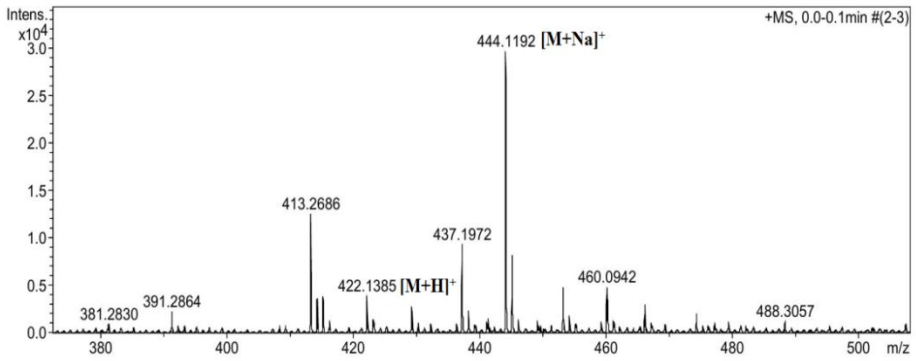

Figure 3.17. *ESI-MS spectrum of* ***L3.***

3.3.2 Infrared Spectroscopy

In the IR spectrum of the **L3** an intense band was observed at 2230 cm^{-1} attributed to *ν*(-CN), of cynao group. Another band at 1695 cm^{-1}, which was assigned to the combined stretching frequency of *ν*(-C=N) and *ν*(-C=O), of the azomethines (-C=N) and carbonyl group of the amide bond of **L3**. An intense band at 3300 cm^{-1} is due to the –NH- vibration of hydrazine group and most intense band at 1540.34 cm^{-1} corresponds to the C-H stretching in H-C=N group in the **L3**. Appearance of these bands suggests the presence of cyano, amide and azomethines functional group in **L3**. [Fig. 3.18]

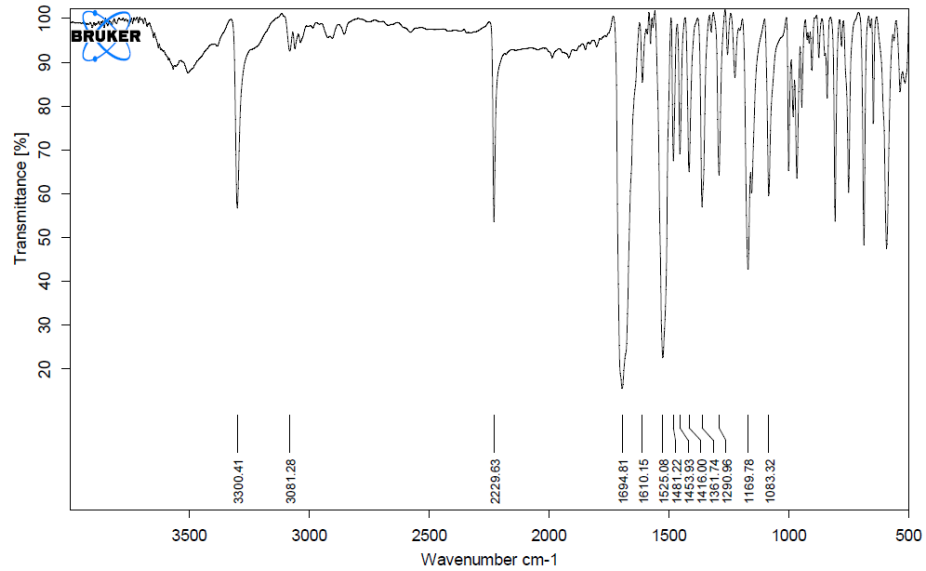

Figure 3.18. *IR spectrum of* ***L3.***

3.3.3 NMR Spectroscopy

NMR spectra of **L3** were recorded in DMSO-d_6 using TMS as an internal

standard. A ^{13}C NMR spectrum for the **L3** is given below in Figure 3.19. The spectrum shows twelve different types of carbons in **L3** molecule. A peak near 159.67 ppm corresponds to carbonyl carbon in compound, peak at 148.06 ppm is attributed to pyridine ring carbon attached to carbonyl group, peak at 118.33 ppm was assigned as cyano group carbon and peak near 147.74 corresponds to the imine carbon. All other peaks show the remaining aromatic carbons.

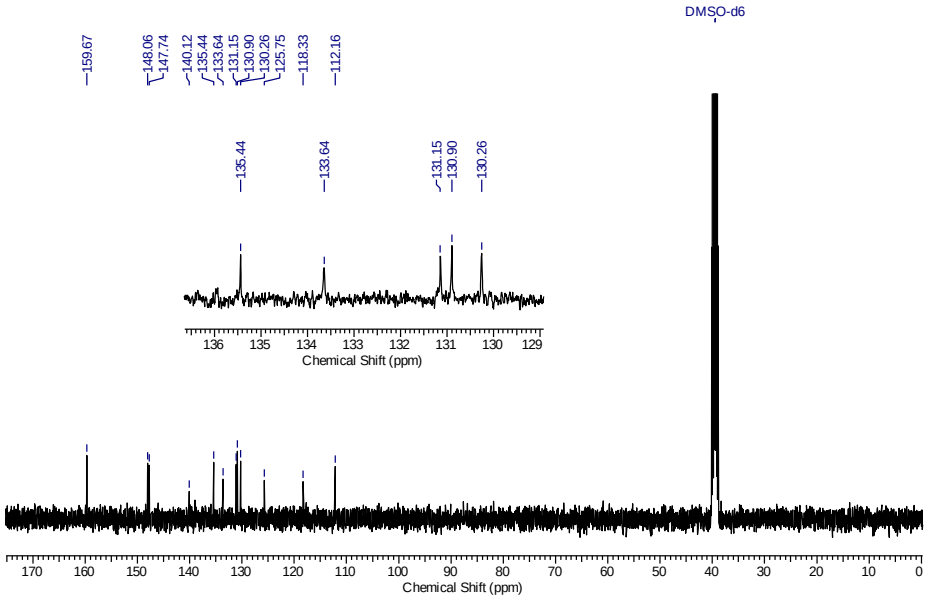

Figure 3.19. *^{13}C NMR spectrum of **L3** in DMSO-d_6.*

The ^{1}H NMR spectrum for the **L3** is given in Figure 3.20, peaks in the region 7.38 to 8.38 ppm were assigned to the proton of aromatic rings. The signals near 12.50 and 8.81 were assigned to the proton of amide –CONH- and imine –CH=N groups, respectively.

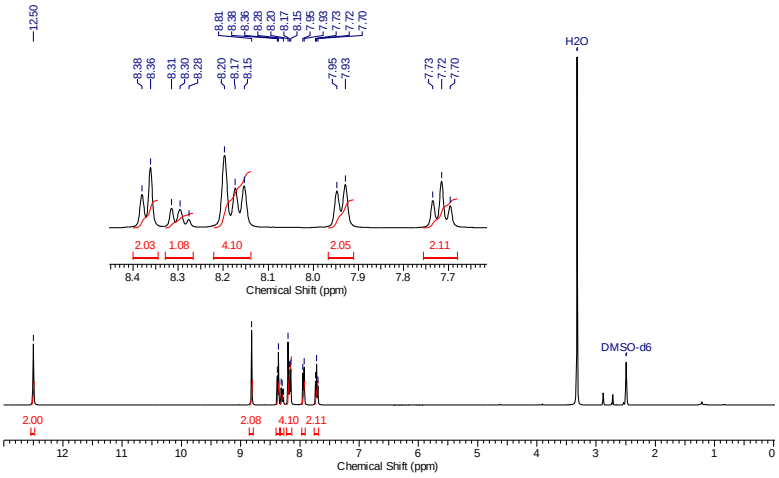

Figure 3.20. *^{1}H NMR spectrum of **L3** in DMSO-d_6.*

3.3.4 Crystal Structure of L3

The white needle shaped crystal of **L3** suitable for X- ray diffraction analysis was obtained by crystallization from dimethylformamide (DMF). A single crystal with approximate dimensions of 0.210 x 0.170 x 0.130 mm^3 was selected for data collection. The molecular structure of the compound with the atom numbering scheme is given in Figure 3.21. The crystallographic data and structure refinement parameters of the compound are given in Table A.1.

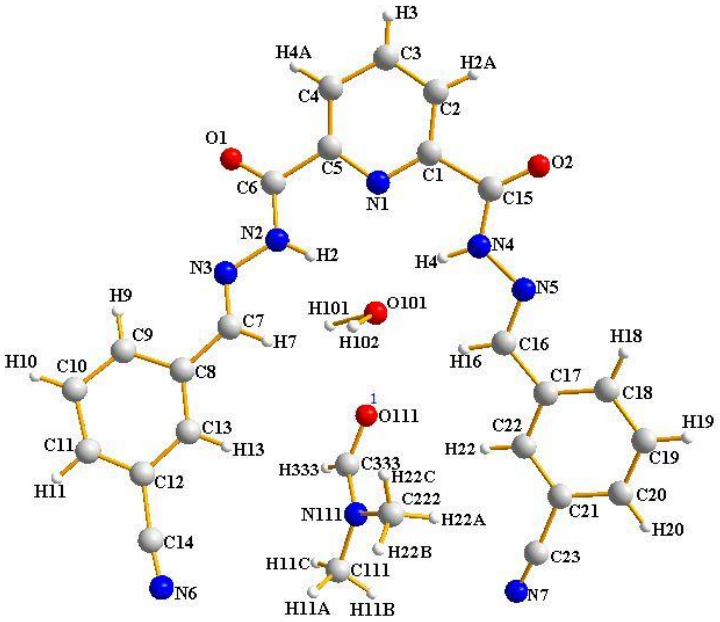

Figure 3.21. *Molecular structure of **L3** with lattice water and DMF mole- cule along with the atom numbering scheme.*

The aroyl hydrazone, **L3** is crystallized into a monoclinic space group *P*ī. The one molecule of **L3** containing a lattice water and dimethyl- formamide molecule is shown in Figure 3.21. In this case the empirical formula of **L3** $C_{26}H_{24}N_8O_4$ can be written as $C_{23}H_{15}N_7O_2.H_2O.C_3H_7NO$.

Figure 3.22 shows the 2-D structure of **L3** with intermolecular interaction. This 2-D structure formed due to two non-conventional H-bonding through C(20)-H(20)…O(1) (2.480 Å) and C(10)-H(10)…O(2) (2.494 Å).

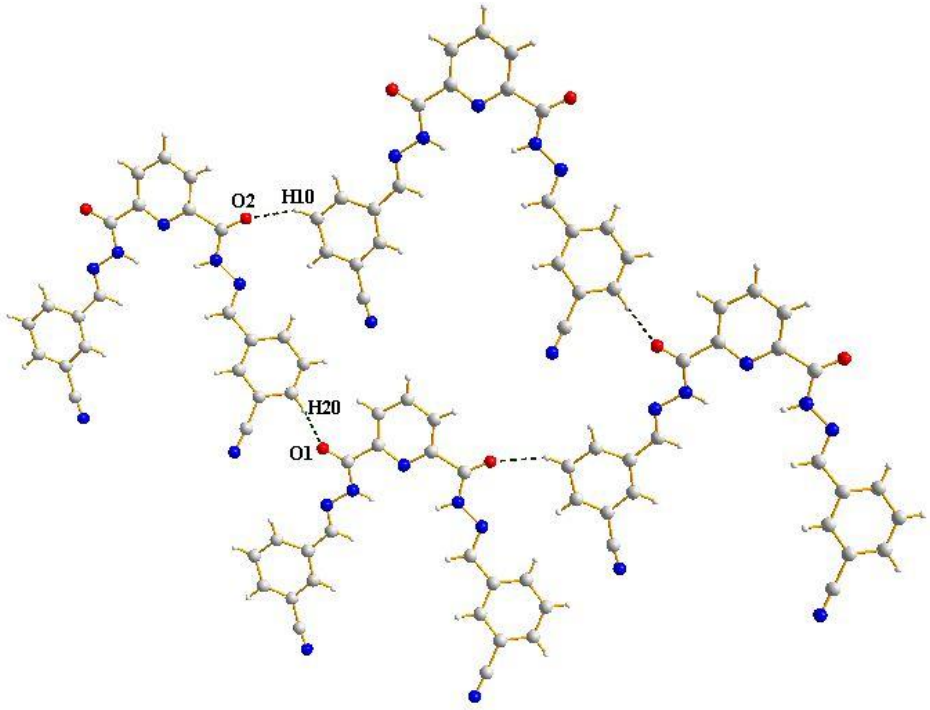

Figure 3.22. *2-D structure of **L3** due to intermolecular interactions.*

A water molecule is linked with two ligand units and a dimethylformamide (DMF) *via* H-bonding interactions. Molecule **1** makes one nonconventional H-bonding with DMF and one conventional hydrogen bond with water molecule which is through carbonyl group oxygen of ligand and hydrogen of water and DMF molecules i.e. C(15)- O(101)-H(102)…O(2) (2.608 Å) and C(222)-H(22C)…O(2) (2.596 Å). Molecule **2** interacted with water oxygen *via* N(2)-H(2)…O(101) (2.173 Å), N(4)-H(4)...O(101) (2.363 Å), C(7)-H(7)...O(101) (2.602 Å) and C(16)-H(16)...O(101) (2.699 Å) and DMF oxygen *via* C(16)-

H(16)…O(111) (2.702 Å). One strong hydrogen bond between hydrogen of water and oxygen of DMF molecule is observed *via* O(101)-H(101)…O(111) (1.843). Molecule **3** formed two interaction with DMF

molecule. These interactions are as follows C(9)-H(9)…O(111) (2.717 Å), C(111)-H(11C)…O(1) (2.525 Å). Molecule **4** has only one interaction with DMF molecule through nitrogen of cyano group of **L3** and methyl hydrogen of DMF C(222)-H(22B)…N(7). These interactions of water and DMF molecules formed 3-D structure of **L3**.

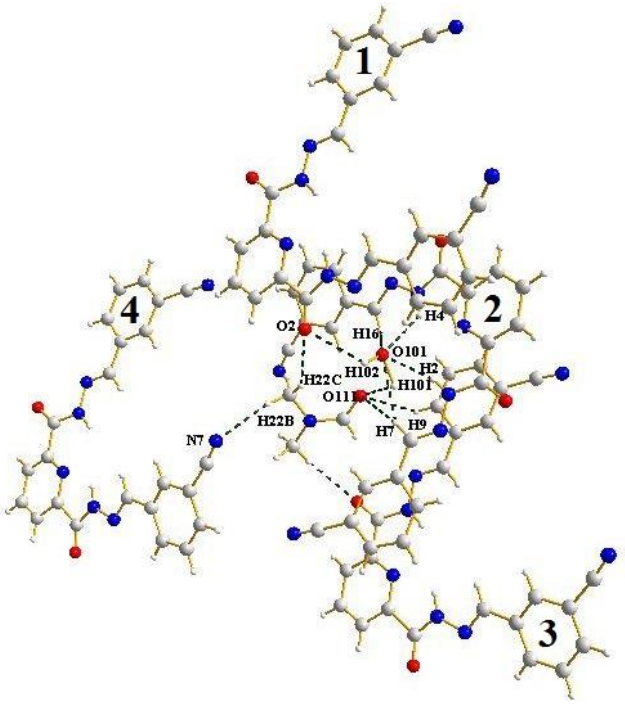

Figure 3.23. *Interactions of water molecule and ethanol molecule with* ***L3****.*

Figure 3.24 shows the packing diagram of the compound **L3** along *c* axis. The packing of molecules in the respective manner in the unit cell is resulted by interactions of lattice solvent molecules and intermolecular Hydrogen bonding.

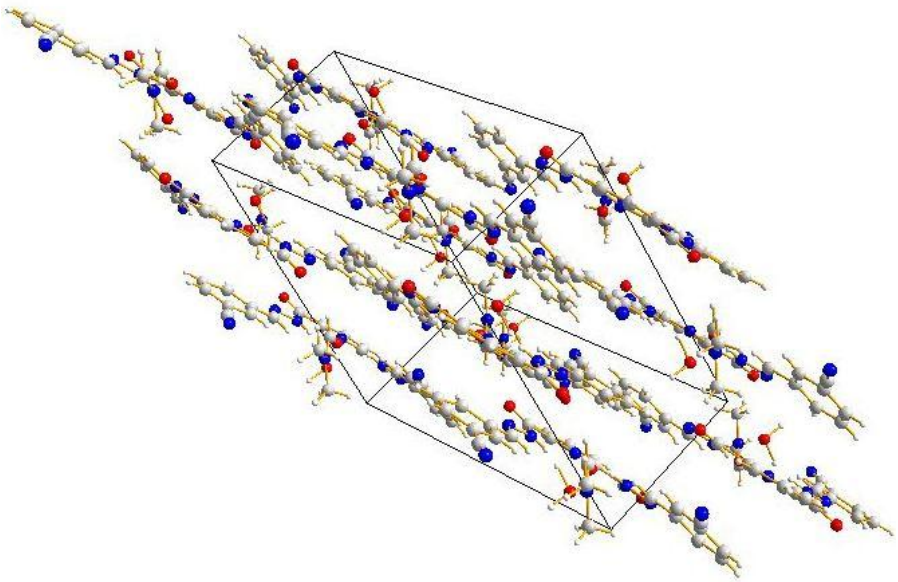

Figure 3.24. *Packing diagram of* ***L3*** *along c axis.*

3. 4 Characterization of L4

3.4.1 Mass Spectrometry

ESI-MS data supports the formation of **L4** with molecular ion peaks at m/z 490.10 and 468.10 which corresponds to the $[M+Na]^+$ and $[M+H]^+$, respectively.

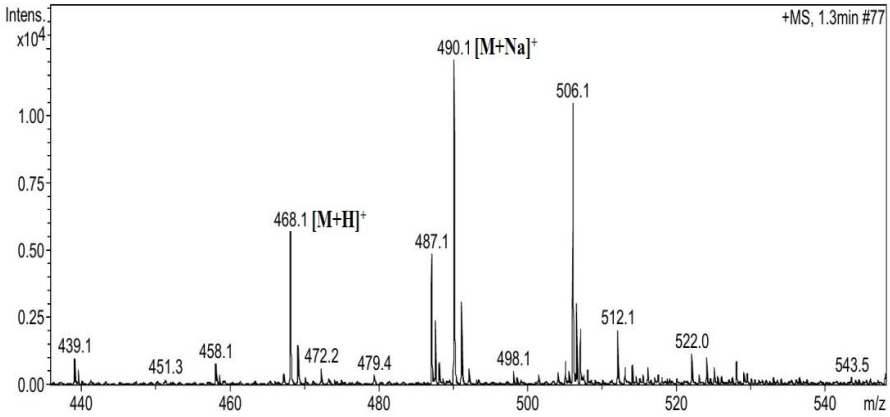

Figure 3.25. *ESI-MS spectrum of* ***L4.***

3.4.2 Infrared Spectroscopy

In the IR spectrum of **L4** the strong and broad IR bands at 3458 and 3472 cm^{-1} attributed to *ν*(-OH) of hydroxyl groups. A most intense band at 1635 cm^{-1}, which was assigned to the stretching frequency, *ν*(-C=N), of the azomethines (-C=N) group. Another band at 3196 cm^{-1} is due to the *ν*(-NH-) of the amide group and

intense band at 1674 cm^{-1} correspond to the *ν*(-C=O), of the carbonyl group of the amide bond. Most intense band at 1585 cm^{-1} correspond to the C-H stretching in H-C=N group in the **L4**. Appearance of these bands suggests the presence of hydroxyl, amide and azomethines functional group in **L4**. [Fig. 3.26]

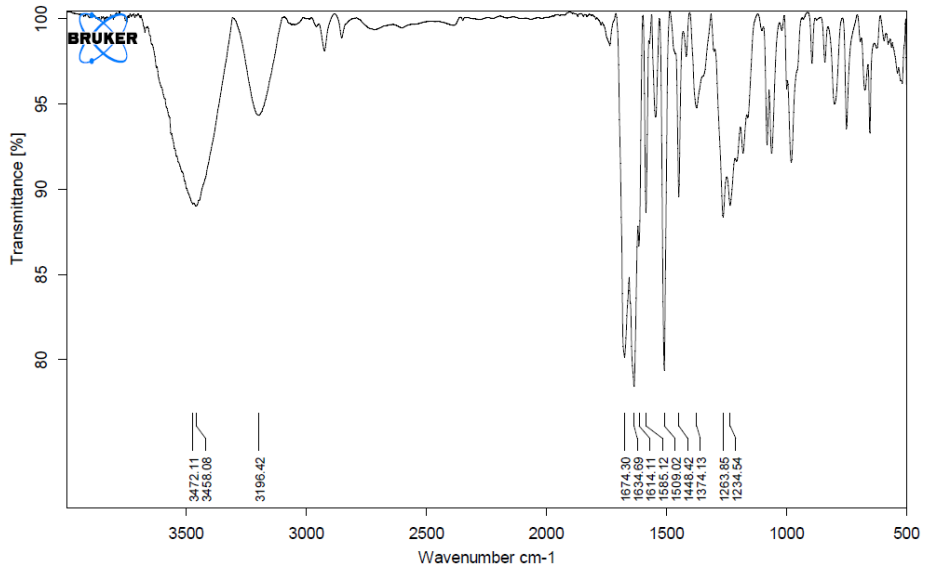

Figure 3.26. *IR spectrum of* ***L4.***

3.4.3 NMR Spectroscopy

NMR spectra of **L4** were recorded in DMSO-d_6 using TMS as an internal standard. A ^{13}C NMR spectrum for the **L4** is given below in Figure 3.27. The spectrum showed eleven different types of carbons in **L4** molecule. A peak near 159.15 ppm corresponds to carbonyl carbon in compound, peaks at 152.00 and 149.26 ppm represents the ortho(o) and para (p)- hydroxyl attached carbon, respectively and peak at 148.12 ppm is attributed to pyridine ring carbon attached to carbonyl group and a peak near 147.78 ppm corresponds to the imine carbon. All other peaks show the remaining aromatic carbons.

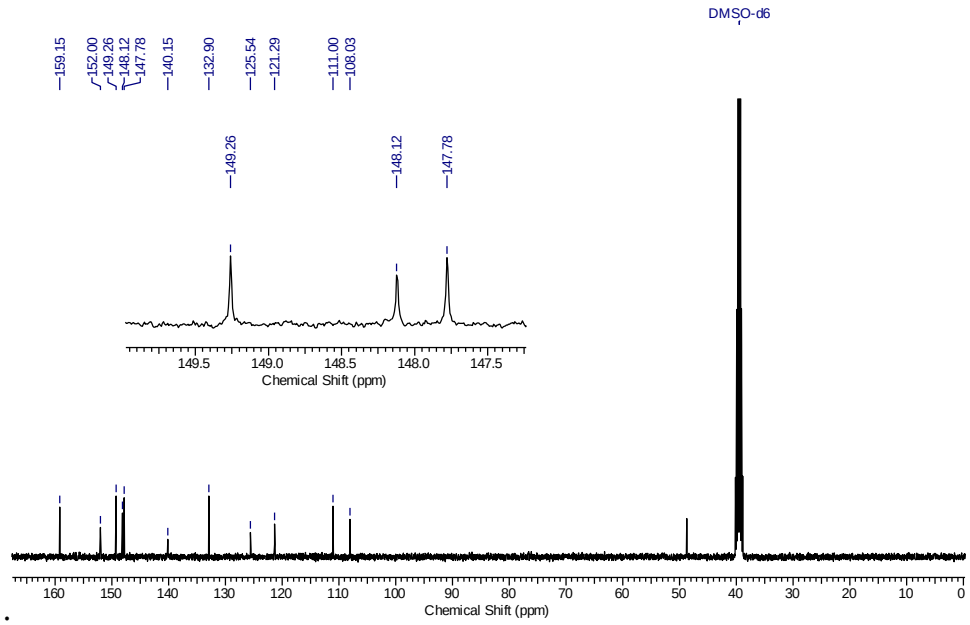

Figure 3.27. *^{13}C NMR spectrum of **L4** in DMSO-d_6.*

The ^{1}H NMR spectrum for the **L4** is given in Figure 3.28. It shows peaks in region 6.43 to 8.38 ppm were assigned to proton of aromatic rings. The signals or peaks near 12.30 and 8.71 were assigned to the proton of amide –CONH- and imine –CH=N groups, respectively.

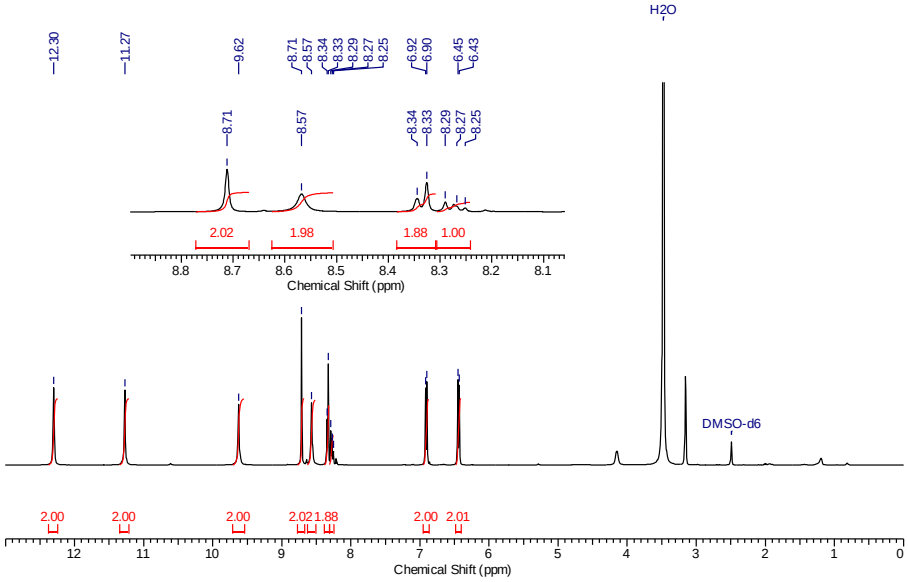

Figure 3.28. *400 MHz ^{1}H NMR spectrum of **L4** in DMSO-d_6.*

3.5.4 Crystal Structure of L4

The yellow color shiny needle shaped crystal of **L4** suitable for X- ray diffraction analysis was obtained by crystallization from a mixture of water and acetone (1:1 v/v). A single crystal with approximate dimensions of 0.210 x 0.170 x 0.130 mm^3 was selected for data collection. The molecular structure of the compound with the atom numbering scheme is given in Figure 3.29. The crystallographic data and structure refinement parameters of the compound are given in Table A.1.

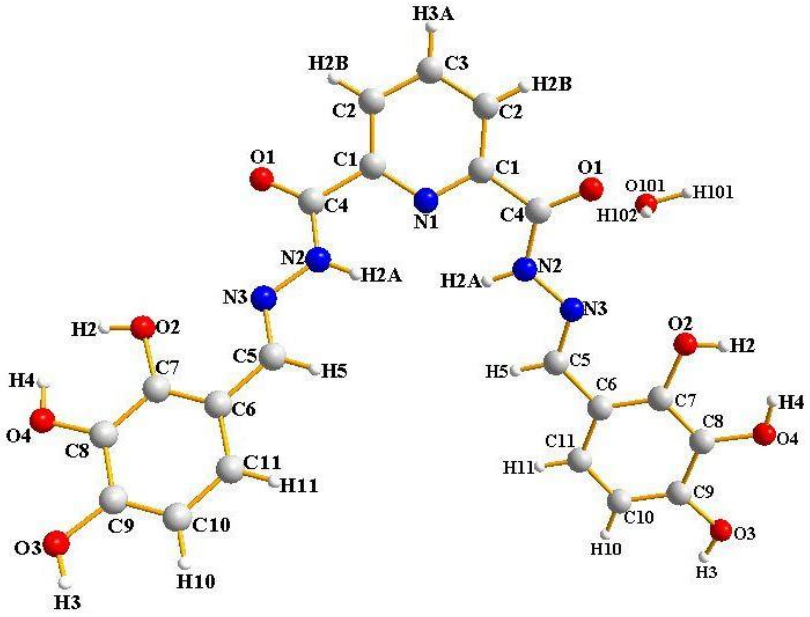

Figure 3.29. *Molecular structure of* ***L4*** *with lattice water molecule along with the atom numbering scheme.*

The aroyl hydrazone, **L4** crystallizes in a monoclinic space group *C* 2/*c*. One molecule of **L4** contains two lattice water [Figure 3.26]. In this case the empirical formula $C_{21}H_{21}N_5O_{10}$ can be written as $C_{21}H_{17}N_5O_8.2H_2O$.

Figure 3.30 shows the 2-D structure of **L3** formed *via* intermolecular interactions. This 2-D structure formed due to non-conventional H-bonding through C(10)-H(10)…O(3) (2.494 Å) and $\pi...\pi$ interactions between D(1)....D(2).

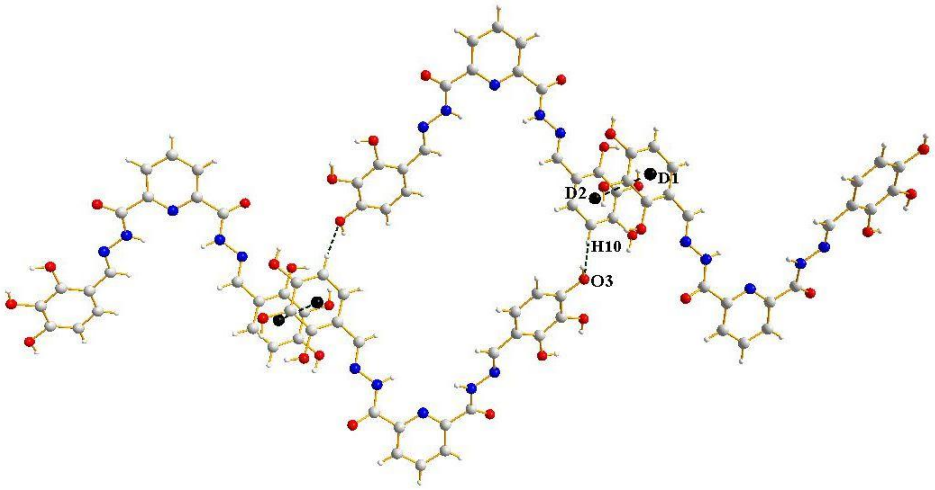

Figure 3.30. *2-D structure of* ***L4*** *due to intermolecular interactions with water molecules.*

In the figure 3.31, one water molecule interacts with four molecule of **L4** via six types of H-bonding interactions O(3)-H(3)...O(101) (1.947 Å) in molecule **1**, O(101)-H(101)…O(4) (2.253 Å) and O(101)-H(101)…O(3) (2.016 Å) in molecule **2**, O(101)-H(102)…O(1) (2.452 Å) in molecule **3** and O(2)-H(2)…O(101) (2.196 Å), O(4)-H(4)…O(101) (1.998 Å) in molecule **4**. These interactions are capable to form the 3-D structure of **L4** molecules.

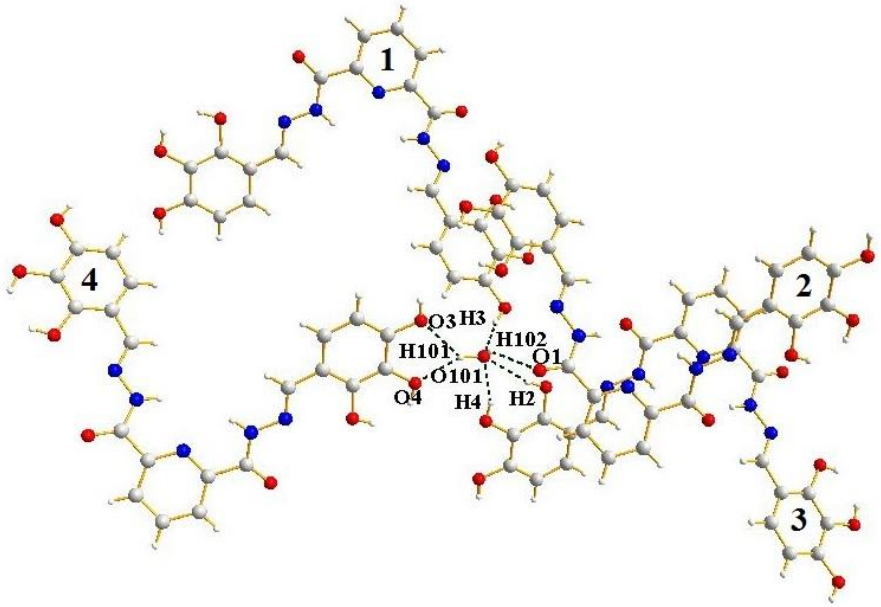

Figure 3.31. *Interactions of water molecule with* ***L4***

Figure 3.32 shows the packing diagram of the compound **L4** along *c* axis. The packing of molecules in the respective manner in the unit cell is resulted by above

interactions given in figure 3.30 and 3.31.

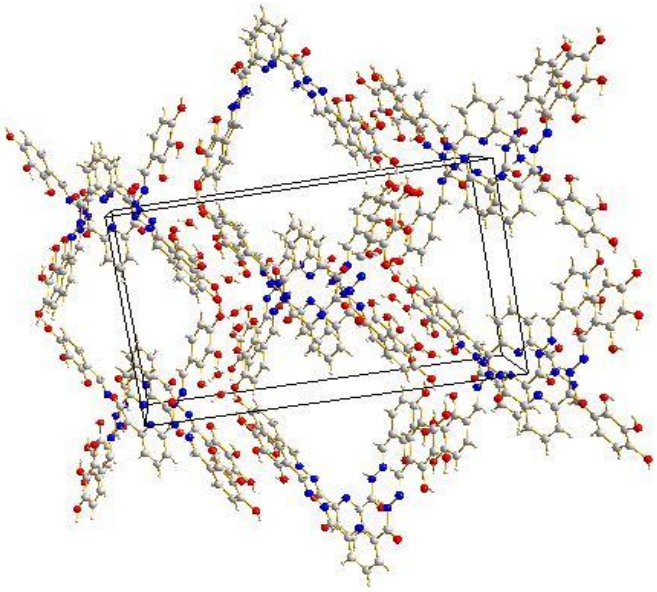

Figure 3.32. *Packing diagram of* ***L4*** *along c axis.*

Chapter 4

Conclusion and Scope for Future Work

Four different aroyl hydrazone ligands have been synthesized by condensation reaction of pyridine-2,6-carbohydrazide with 4-phenyl- benzaldehyde, 4-(4-pyridyl)benzaldehyde, 3-cyanobenzaldehyde or 2,3,4-trihydroxybenzaldehyde. In most cases, the yield was more than 80%. X-ray quality single crystals of all the four aroyl hydrazones were grown in a mixture of solvents. Their molecular structures were confirmed by single crystal X-ray diffraction studies. The studied aroyl hydrazones have been crystallized in hydrated forms. The water molecules incorporated into the crystal can be derived either from the crystallization solution or from the air. The single crystal X-ray diffraction studies of the aoryl hydrazone also reveal that aroyl hydrazones exist in amido form in the solid state and also it was found that all studied hydrazones adopts the E configuration around N=C group in the solid state. The association modes in the studied crystals are dominated by strong hydrogen bonds of the N-H...O type involving the amide group as a proton donor. The water-hydrazone interactions are among the strongest ones in the analyzed crystals. Apart from strong hydrogen bonding, there are some other weak interaction which are as follows (1) **L1** shows C-H…O and C-H…π interaction, (2) **L2** shows C-H...O, C-H...N and C-H...π contacts, (3) **L3** shows CH...N and C-H...O, (4) **L4** shows C-H...O and π…π stacking interactions.

Aroyl hydrazones show a broad spectrum of applications in pharmaceutical and industrial fields. The aroyl hydrazones show a variety of biological activities with potential uses in antibacterial, antifungal and anticancer studies [25-29]. In addition, their varied coordinating behavior makes them interesting candidates for metal-based drugs [30]. Hydrazones and their metal complexes have found practical use in chemical processes like non linear optics(NLO), sensors etc. Donor-π-Acceptor type aroyl hydrazones play an important role in the second harmonic generation efficiency. The wide transparency window in the visible region makes them ideal candidates for NLO applications [31-33].

Synthesis and characterization of some new aroyl hydrazone open a new gate-way in the field of coordination chemistry. These are versatile ligands with multiple donor atoms. Further attempts would be made to carry out a systematic study on the metal complex of these aroyl hydrazones. We will try to prepare some metal complexes of these ligands and also look forward for their further applications in the field of medicinal, catalytic, analytical and nonlinear optics.

APPENDIX-A

Table A.1. Crystal Data and Structure Refinement Parameters for Aroyl hydrazone Ligands (**L1-L4**).

Identification Code	**L1**	**L2**	**L3**	**L4**
Empirical formula	C_{33} H_{27} N_5O_3	$C_{33}H_{31}N_7O_4$	$C_{26}H_{24}N_8O_4$	$C_{21}H_{21}N_5O_{10}$
Formula weight	541.59	589.65	512.51	503.42
Temperature (K)	150(2)	150(2)	293(2)	293(2)
Wavelength (Å)	1.5418	0.71073	1.5418	1.5418
Crystal system, space group	Triclinic, *P*ī	Monoclinic, *P* 21/*c*	Triclinic, *P*ī	Monoclinic, *C* 2/*c*
Unit Cell Parameter				
a (Å)	10.1674(3)	23.0525(11)	7.6087(17)	23.281(5)
b (Å)	10.3568(5)	10.4701(5)	13.553(3)	13.731(3)
c (Å)	14.4668(6)	12.7208(7)	14.344(3)	8.5073(15)
α (deg.)	71.840(4)	90	115.81(2)	90
β (deg.)	69.606(4)	103.858(5)	97.686(17)	99.538(19)
γ (deg.)	86.751(3)	90	97.698(18)	90
V (Å3)	1354.46(10)	2980.9(3)	1288.7(5)	2682.0(9)

Z, d_{calcd}(mg/m^3)	2, 1.328	4, 1.314	2, 1.316	8, 1.247
Absorption coefficient, μ (mm^{-1})	0.703	0.089	0.769	0.866
F(000)	568	1240	532	1048
Crystal size (mm^3)	0.230 x 0.170 x 0.130	0.210 x 0.170 x 0.130	0.260 x 0.220 x 0.170	0.210 x 0.170 x 0.130
Crystal color and form	white needle	yellow needle	white needle	yellow needle
θ range (deg.)	3.431 to 71.354	2.895 to 25.000	3.505 to 39.989	3.751 to 39.986
Index ranges	-12<=h<=8, -12<=k<=12, -17<=l<=16	-27<=h<=27, -16<=k<=11, -15<=l<=15	-6<=h<=5, -11<=k<=11, -11<=l<=11	-19<=h<=19, -11<=k<=11, -7<=l<=7
Reflections collected / unique	8948 / 5142 [$R_{(int)}$ = 0.0145]	20316 / 5228 [$R_{(int)}$ = 0.0792]	3095 / 1566 [$R_{(int)}$ = 0.0362]	3191 / 821 [$R_{(int)}$ = 0.0833]
Max. and min. transmission	1.00000 and 0.83320	1.00000 and 0.40262	1.00000 and 0.73015	1.00000 and 0.45412
Data/restraints / parameters	5142 / 0 / 374	5228 / 0 / 410	1566 / 0 / 346	821 / 2 / 176
GOF, F^2	1.023	1.137	2.487	1.082
R_1, wR_2 [I>2σ(I)]	R_1 = 0.0349, wR_2 = 0.0956	R_1 = 0.0585, wR_2 = 0.1566	R_1 = 0.2493, wR_2 = 0.5641	R_1 = 0.0814, wR_2 = 0.2222
R_1, wR_2 (all data)	R_1 = 0.0363, wR_2 = 0.0973	R_1 = 0.0894, wR_2 = 0.1711	R_1 = 0.2702, wR_2 = 0.5835	R_1 = 0.1024, wR_2 = 0.2414

GOF, F^2	1.023	1.137	2.487	1.082
Absorption correction	Semi-empirical from equivalents	Semi-empirical from equivalents	Semi-empirical from equivalents	Semi-empirical from equivalents
Refinement method	Full-matrix least-squares on F^2	Full-matrix least-squares on F^2	Full-matrix least-squares on F^2	Full-matrix least-squares on F^2

Table A.2. Selected Bond Distances for Aroyl Hydrazone Ligands (**L1-L4)**.

Bond Length (Å)	**L1**	**L2**	**L3**	**L4**
N(1)-C(5)	1.335(4)	1.340(3)	1.344(3)	1.345(3)
C(5)-C(6)	1.502(5)	1.500(4)	1.509(4)	1.497(4)
O(1)-C(6)	1.225(3)	1.227(3)	1.169(2)	1.221(2)
N(2)-C(6)	1.347(5)	1.338(3)	1.348(3)	1.330(7)
N(2)-N(3)	1.376(3)	1.376(5)	1.386(3)	1.381(6)
N(3)-N(7)	1.284(5)	1.264(4)	1.237(3)	1.293(4)
C(7)-C(8)	1.459(6)	1.461(3)	1.449(4)	1.450(3)
N(1)-C(1)	1.334(4)	1.337(3)	1.323(5)	1.345(3)
C(1)-C(20)	1.501(4)	1.504(4)	1.591(2)	1.497(4)
O(2)-C(20)	1.228(3)	1.232(5)	1.168(3)	1.221(2)
C(20)-N(4)	1.351(4)	1.338(4)	1.306(3)	1.330(7)
N(4)-N(5)	1.381(2)	1.380(6)	1.398(3)	1.381(6)

N(5)-C(21)	1.280(4)	1.272(4)	1.301(3)	1.293(4)
C(21)-C(22)	1.463(4)	1.458(4)	1.484(4)	1.450(3)

Table A.3. Selected Bond Angles for Aroyl Hydrazones Ligands (**L1-L4)**.

Bond Angle (º)	**L1**	**L2**	**L3**	**L4**
N(1)-C(5)-C(6)	116.69(9)	116.72(2)	113.13(3)	116.55(9)
C(5)-C(6)-O(1)	122.37(10)	120.93(4)	118.90(3)	121.53(11)
O(1)-C(6)-N(2)	124.88(11)	124.31(6)	126.54(2)	124.55(5)
C(5)-C(6)-N(2)	112.75(9)	114.66(4)	114.50(3)	113.92(5)
C(6)-N(2)-N(3)	121.06(9)	119.15(3)	116.96(4)	119.38(6)
N(2)-N(3)-C(7)	114.06(9)	116.65(3)	116.34(2)	116.07(3)
N(3)-C(7)-C(8)	121.95(10)	121.59(4)	125.47(3)	121.41(8)
N(1)-C(1)-C(20)	117.27(9)	117.12(5)	120.05(4)	116.55(9)
C(1)-C(20)-O(2)	121.39(10)	120.37(7)	124.93(2)	121.53(11)
O(2)-C(20)-N(4)	124.55(10)	124.08(3)	125.60(3)	124.55(5)
C(20)-N(4)-N(5)	118.63(9)	119.69(7)	123.03(3)	113.92(5)
N(4)-N(5)-C(21)	115.29(9)	116.23(8)	113.84(3)	119.38(6)
N(5)-C(21)-C(22)	120.63(10)	123.21(6)	119.76(4)	116.07(3)
C(1)-N(1)-C(5)	117.64(10)	116.71(9)	114.89(2)	114.89(8)

Table A.4. Selected Torsion Angle for Aroyl Hydrazone Ligands (**L1-L4**).

Torsion Angle (º)	**L1**	**L2**	**L3**	**L4**
N(1)-C(5)-C(6)-N(2)	-14.19(14)	6.98(2)	-16.12(4)	18.49(4)
N(1)-C(5)-C(6)-O(1)	166.38(10)	-176.62(4)	166.54(2)	-160.72(4)
C(5)-C(6)-N(2)-N(3)	-178.65(9)	174.58(6)	-175.94(3)	179.64(5)
O(1)-C(6)-N(2)-N(3)	0.76(17)	-1.67(4)	1.16(5)	-1.18(3)
C(6)-N(2)-N(3)-C(7)	174.93(10)	-174.84(3)	-177.94(5)	-177.63(5)
N(2)-N(3) -C(7)-C(8)	178.33(9)	178.89(3)	177.02(8)	-177.87(5)
N(1)-C(1)-C(20)-N(4)	-19.33(13)	16.65(8)	-6.21(2)	18.49(7)
N(1)-C(1)-C(20)-O(2)	161.96(10)	-164.48(5)	175.74(6)	-160.72(8)
C(1)-C(20)-N(4)-N(5)	-170.07(8)	175.92(7)	179.54(5)	179.64(3)
O(2)-C(20)-N(2)-N(3)	8.59(16)	-2.91(4)	-2.43(4)	-1.18(7)
C(20)-N(4)-N(5)-C(21)	175.51(9)	-178.30(2)	174.50(2)	-177.63(8)
N(4)-N(5)-C(21)-C(22)	-171.89(9)	178.55(3)	178.23(7)	-177.87(8)

Table A.5. Hydrogen Bonding Interactions for all the studied Aroyl Hydrazone Ligands (**L1-L4**).

Ligand	**Interaction**	**d_{D-H} (Å)**	**$d_{H...A}$ (Å)**	**∠D-H...A (°)**
L1	O(111)-H(11B)...N(3)	0.850(3)	2.216(3)	160.71(9)
	O(111)-H(11B)...O(1)	0.850(3)	2.472(3)	125.57(3)

	N(2)-H(2)...O(111)	0.880(4)	2.544(3)	125.60(8)
	N(4)-H(4)...O(111)	0.880(4)	2.192(3)	159.00(10)
	C(21)-H(21)...O(111)	0.950(3)	2.417(3)	148.42(7)
	O(111)-H(11A)...O(2)	0.850(3)	2.227(3)	153.66(7)
L2	O(111)-H(111)...O(222)	0.835(2)	1.943(3)	162.49(5)
	O(111)-H(222)...O(1)	0.912(3)	2.086(3)	159.37(10)
	N(2)-H(2)...O(111)	0.880(2)	2.263(3)	146.82(3)
	N(4)-H(4)...O(111)	0.880(2)	2.214(4)	156.28(3)
	C(7)-H(7)...O(111)	0.950(3)	2.263(4)	134.15(3)
	C(20)-H(20)...O(111)	0.950(3)	2.502(3)	145.97(4)
	C(3)-H(3)...O(222)	0.950(3)	2.655(4)	133.99(3)
	C(9)-H(9)...O(222)	0.950(3)	2.570(3)	172.38(13)
	O(222)-H(101)...N(3)	0.997(5)	2.487(10)	126.67(10)
	O(222)-H(101)...O(2)	0.997(5)	1.883(6)	158.20(8)
	C(20)-H(20)...N(7)	0.950(3)	2.717(11)	142.77(4)
	C(29)-H(29)...N(7)	0.950(3)	2.717(6)	142.77(10)
L3	N(2)-H(2)...O(101)	0.860(4)	2.173(5)	159.13(12)
	N(4)-H(4)...O(101)	0.860(4)	2.363(5)	131.55(3)

	C(16)-H(16)...O(101)	0.930(3)	2.699(4)	120.45(3)
	N(7)-H(7)...O(101)	0.930(3)	2.602(5)	146.20(3)
	O(101)-H(102)...O(2)	1.034(4)	2.608(5)	106.67(10)
	C(9)-H(9)...O(111)	0.930(3)	2.717(8)	116.75(8)
	C(111)-H(11C)...O(111)	0.960(3)	2.525(4)	161.56(7)
	O(222)-H(22B)...N(7)	0.960(3)	2.631(2)	164.25(10)
	O(222)-H(22B)...N(2)	0.960(3)	2.596(2)	141.45(6)
	C(16)-H(16)...O(111)	0.930(2)	2.702(2)	148.52(6)
	C(10)-H(10)...O(2)	0.930(2)	2.494(2)	148.05(7)
	C(16)-H(16)...O(111)	0.930(3)	2.702(2)	148.52(3)
L4	O(16)-H(16)...O(101)	0.820(2)	2.196(2)	158.40(4)
	O(4)-H(4)...O(101)	0.820(2)	1.998(2)	158.40(4)
	O(3)-H(3)...O(101)	0.820(2)	1.947(2)	164.72(4)
	O(101)-H(102)...O(01)	0.648(4)	2.452(2)	140.03(3)
	O(101)-H(101)...O(4)	0.971(3)	2.253(2)	143.34(3)
	O(101)-H(101)...O(3)	0.971(3)	2.016(3)	139.11(4)
	C(10)-H(10)...O(3)	0.930(3)	2.526(4)	149.90(4)
	C(5)-H(5)...O(1)	0.930(3)	2.238(3)	147.90(4)

	N(2)-H2A)...O(1)	0.860(3)	2.580(2)	140.18(3)

Table 1.6 $\pi...\pi$ and $CH...\pi$ Interactions in the studied Aroyl Hydrazone Ligands.

Ligand	**Interaction**	d (Å)
L1	C(23)-H(23)...D(1)[#]	3.579(10)
	C(30)-H(30)...D(2)[#]	3.579(9)
L2	C(2)-H(2A)...D(1)[*]	3.672(10)
L4	D(1)[a]...D(2)[b]	3.377(6)

D(1) is the dummy atom between the carbon C(14), C(15), C(16), C(17), C(18), C(19) and D(2) is the dummy atom between C(28), C(29), C(30), C(31), C(32), C(33).

* D(1) is the dummy atom between C(21), C(22), C(23), C(24), C(30), C(31).

[a] D(1) is the dummy atom between C(6), D(7), D(8), D(9), D(10), D(11).

[b] D(2) is the dummy atom between C(6), D(7), D(8), D(9), D(10), D(11).

REFERENCES

1. Sagiura, M.; Kabayashi S. *Angew. Chem.* **2005**, *44*, 5176−5186.
2. Friestad, G.K. *Eur. J. Org. Chem.* **2005**, 3157−3172.
3. Friestad, G.K.; Draghici, C.; Soukri, M.; Qin, J. *J. Org. Chem.* **2005**, *70*, 6330−6338.
4. Samanta, B.; Chakraborty, J.; Shit, S.; Batten, S.R.; Jensen, P.; Masuda, J.D.; Mitra, S. *Inorg. Chim. Acta* 2007, *360*, 2471−2484.
5. Banerjee, S.; Mondal, S.; Sen, S.; Das, S.; Hughes, D.L.; Rizzoli, C.; Desplanches, C.; Mandal, Ch.; Mitra, S. *Dalton Trans.* **2009**, 6849−6860.
6. Sing, R.B. *Talanta* **1982**, *29*, 77−84.
7. Katyal, M.; Dutt, Y. *Talanta* **1975**, *22*, 151−166.
8. Narang, R.; Narasimhan, B.; Sharma, S. *Curr. Med. Chem.* **2012**, *19 (4)*, 569−612.
9. Xin, S.; Ivan, A. *Chem. Soc. Rev.* **2014**, 43, 1963.
10. Naseema, K.; Sujith, K.V.; Manjunatha, K.B.; Kalluraya, B.; Umesh, G.; Rao, V. *Optic. Laser Tech.* **2010**, *42*, 741.
11. Cariati, F.; Caruso, U.; Centore, R.; Marcolli, W.; Maria, A.D.; Panunzi, B.; Roviello, M.A.; Tuzi, A. *Inorg. Chem.* **2002**, 41, 6597.
12. Hearn, M.J.; Cynamon, M.H. *J. Antimicrob. Chemother.* **2004**, *53(2)*, 185–191.
13. Przybylski, P.; Huczynski, A.; Pyta, K.; Brzezinski, B.; Bartl, F. *Curr. Org. Chem.* **2009**, *13(2)*, 124–148.
14. Walcourt, A.; Loyevsky, M., Lovejoy, D.B.; Gordeuk, V.R., Richardson, D.R. *Int. J. Biochem. Cell Biol*. **2004**, *36*, 401-407.
15. Xiang, Y.; Tong, A.J.; Jin, P.Y.; Ju, Y. *Org. Lett.* **2006**, *8*, 2863.
16. Krishna, D.G.; Devanna, N.; Chandrasekhar, K.B. *Int. J. Pharm. Bio. Sci.* **2011**, *1 (1)*, 1-8.
17. Thilagavathi, N.; Manimaran, A.; Priya, N.P.; Sathya, N.; Jayabalakrishnan, C. *Appl. Organometal. Chem*. **2010**, *24*, 301.

18. Manas, S.; Marina, V.; Kirillova, M.; Fátima, C.; Guedes, D.S.; Cai-Ming, L.; Pombeiro, A.J.L. *Dalton Trans.* **2013**, *42*, 16578.
19. Manas, S.; Luísa M.D.; Martins, R. S.; Fátima, C.; Guedes, D.S.; Elisabete, C.B.; Alegria, A.; Cai-Ming, L.; Pombeiro, A.J.L. *Dalton Trans.* **2014**, *43*, 3966.
20. Mizar, A.; Guedes, D.S.; Kopylovich, M.N.; Mukherjee, S.; Mahmudov, K.T.; Pombeiro, A.J.L. *Eur. J. Inorg. Chem.* **2012**, 2305.
21. Dipali, S.; Aurkie, R.; Guillaume, P.; Corrado, R.; Georgina, M. R.; Carlos, J.G.; Sandra, S.; Sebastian, B.; Samiran, M. *Inorg. Chem.* **2011**, *50*, 8326–8339.
22. Guoliang, G.U.; Ming, L.U. *E. J. Chem.* **2011**, *8(1)*, 449-452.
23. Alyar, S.; Karacan, N. *J. Enzyme Inhib. Med. Chem*. **2009**, *24*, 986 –992.
24. Sonmez, M.; Sogukomerogullari, H.G.; Oztemel, F.; Berber, I. *Med. Chem. Res.* **2014**, *23*, 3451–3457.
25. Hollo, B.; Magyari, J.; Radovanovic, V.Z.; Vuckovic, G.; Tomic, Z.D.; Szilagyi, I.M.; Pokol, G.; Szecsenyi, K.M. *Polyhedron* **2014**, *80*, 142.
26. Parrilha, G.L.; Vieira, R.P.; Rebolledo, A.P.; Mendes, I.C.; Lima, L.M.; Barreiro, E.J.; Piro, O.E.; Castellano, E.E.; Beraldo, H. *Polyhedron* **2011**, *30*, 1891.
27. Nfor, E.N.; Husian, A.; Majoumo-Mbe, F; Njah, I.N.; Offiong, O.E.; Bourne, S.A. Polyhedron **2013**, *63*, 207.
28. Dandawatea, P.; Vemurib, K.; Khan, E.M.; Sritharan, M.; Padhye, S. Carbohydr. Polym. **2014**,*108*, 135.
29. Krishnamoorthy, P.; Sathyadevi, P.; Butorac, R.R.; Cowley, A.H.; Bhuvanesh, N.S.P., Dharmaraj, N. *Dalton Trans.* **2012**, *41*, 6842.
30. Ebrahimipour, S.Y.; Sheikhshoaie, I.; Crochet, A.; Khaleghi, M.; Fromm, M. *J. Mol. Struct.* **2014**, *1072*, 267.
31. Babu, G.A., Ramasamy, R.P.; Ramasamy, P.; Natarajan, S. *J. Cryst. Growth* **2009**, *311*, 3461.
32. Henari, F.Z.; Patil, P.S. *Optics and Photonics Journal* **2014**, *4*, 182.
33. Reshak, A.H.; Kamarudin, H.; Auluck, S. *J. Phys. Chem.* **2012**, *116* 4677.